

## Enabling Interactive Infrastructure with Body Channel Communication

VIRAG VARGA, ETH Zurich & Disney Research, Switzerland

GERGELY VAKULYA, ETH Zurich & Disney Research, Switzerland

ALANSON SAMPLE, Disney Research, USA

THOMAS R. GROSS, ETH Zurich, Switzerland

Body channel communication (BCC) uses the human body to carry signals, and therefore provides communication and localization that are directly tied to human presence and actions. Previous BCC systems were expensive, could operate only in a laboratory, or only focused on special use cases. We present here an end-to-end BCC system that is designed for ambient intelligence. We introduce the BCC infrastructure that consists of portable devices (e.g., a simple sphere), mobile devices (e.g., a smartwatch-like wristband), and stationary devices (e.g., floor/wall tiles). We also describe the core technology that is used in each of these units. The TouchCom hardware-software platform is a simple transceiver with software-centered processing. The focus on software (even the implementation of the physical layer is based on software) allows the adaptivity that is necessary to operate a BCC-based system in practice. The paper describes the design and a prototype implementation of the TouchCom-based interactive infrastructure and provides evidence that this BCC infrastructure works for different persons and different setups. The system provides moderate bandwidth (about 3.5 kb/s) that is suitable for several usage scenarios like games, localization, and identification. The implemented demonstrations illustrate the benefits these applications gain when touching an object is tied to communication.

CCS Concepts: • **Computer systems organization** → *Embedded systems*; • **Human-centered computing** → *Ubiquitous and mobile computing systems and tools; Mobile devices*;

Additional Key Words and Phrases: body channel communication; capacitive coupling; human-computer interaction; wearable devices; smart floor

### ACM Reference Format:

Virag Varga, Gergely Vakulya, Alanson Sample, and Thomas R. Gross. 2017. Enabling Interactive Infrastructure with Body Channel Communication. *Proc. ACM Interact. Mob. Wearable Ubiquitous Technol.* 1, 4, Article 169 (December 2017), 29 pages. <https://doi.org/10.1145/3161180>

---

We thank Stefan Mangold for leadership in the early stages of this project and for helping us to understand the potential of body channel communication. Bob Sumner provided guidance and, together with Mattia Ryffel, allowed us to base one of our demonstrators (MusicBand) on one of their earlier systems. Giorgio Corbellini, Yawhwei Lam, Stefan Schmid, and Chouchang (Jack) Yang helped with comments and suggestions at one point during the design of the BCC system presented here. Gaurav Chaurasia, Henning Zimmer, Christian Schumacher, Yeara Kozlov, Marc Wyss, and Lito Kriara were enthusiastic participants in various tests while the system was under development and provided valuable feedback. Alessia Marra, Maurizio Nitti, Kyna McIntosh, and James Krahe designed and revised the artwork shown here and in our supplementary video. We also thank all additional users who participated in our evaluation.

Authors' addresses: Virag Varga, ETH Zurich & Disney Research, Zurich, Switzerland, [virag.varga@disneyresearch.com](mailto:virag.varga@disneyresearch.com); Gergely Vakulya, ETH Zurich & Disney Research, Zurich, Switzerland; Alanson Sample, Disney Research, Pittsburgh, USA; Thomas R. Gross, ETH Zurich, Zurich, Switzerland.

---

Permission to make digital or hard copies of all or part of this work for personal or classroom use is granted without fee provided that copies are not made or distributed for profit or commercial advantage and that copies bear this notice and the full citation on the first page. Copyrights for components of this work owned by others than the author(s) must be honored. Abstracting with credit is permitted. To copy otherwise, or republish, to post on servers or to redistribute to lists, requires prior specific permission and/or a fee. Request permissions from [permissions@acm.org](mailto:permissions@acm.org).

© 2017 Copyright held by the owner/author(s). Publication rights licensed to Association for Computing Machinery.

2474-9567/2017/12-ART169 \$15.00

<https://doi.org/10.1145/3161180>

## 1 INTRODUCTION

Interaction is a central theme of ubiquitous computing. Body channel communication (BCC) supports interactions where natural touch events enable communication: whenever a person touches a physical object, this object becomes the interface of an environment that is sensitive and responsive to its occupants. For example, a user's smartwatch may contain a key that is communicated via BCC when this person touches the lock of a safe. Then receiving the key (a data transfer) implies that the person that carried the key device touched the lock and access can be granted. Multiple participants can be supported as well: a door is opened only when two key holders together touch the lock, and each person's personal key device logs the identity of the persons that were present.

BCC provides a seamless communication technology for human-centered connectivity: it can connect multiple on-body and/or external devices by using the human body as transmission medium. That is, the communication is strictly limited to close proximity or physical contact of the body which makes it similar to passive RFID tags, contactless smart cards, and NFC solutions. Nevertheless, BCC differs from these technologies because it does not require a dedicated contact point. Once the wearable is attached to its user, the communication works across his/her whole body. When communication is possible, the participants can send and receive data, just as they can do when working with a wireless (WiFi) or wired connection. BCC allows moderate data rates (usually a few kb/s) that are well-suited to exchange control information, e.g., a user's ID or status updates.

While the potential of BCC for interactive environments has long been known, actual usage of BCC-based systems has so far been restricted to laboratories. In this paper we describe a BCC system that supports constructs that can serve as foundation for ambient intelligence: mobile devices (e.g., a smartwatch-like wristband), portable devices, and stationary devices (e.g., wall/floor tiles that contain contacts to identify or track a user). All these units are built upon the TouchCom core: a bidirectional half-duplex transceiver that is based on the capacitive coupling model and allows communication using the human body as medium.

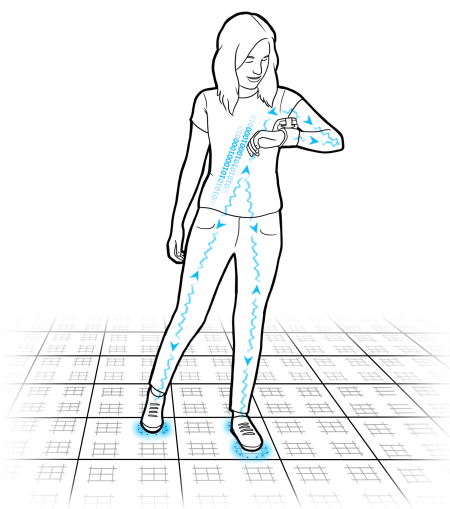


Fig. 1. An example of how body channel communication (BCC) infrastructure can be utilized for ambient intelligence: a person is identified by the floor and receives location-specific information on her BCC smartwatch as she walks on the floor.

The presented BCC infrastructure provides an example how communication and interaction could be smoothly and seamlessly integrated into the every day life in a non-intrusive manner. The advantages of the novel BCC system discussed here are threefold: it can serve as a tracking, user localization, and identification system, as an interactive surface for physical games, or as a general ubiquitous human-centered networking solution. BCC limits the range of interactions – participants must make physical contact or at least be very close (on the order of cm) – and thereby avoids many of the disadvantages of (radio) wireless technology, and this feature enables context-aware, human-centric human-computer interaction design for future business and leisure environments. We implemented a prototype to investigate a number of design parameters and to allow a preliminary assessment of the strengths and weaknesses of this approach.

The paper starts with reviewing the background of smart environments and the different body channel communication systems (Section 2). This discussion leads to Section 3, in which we point out the lack of portable, end-to-end BCC prototype systems and

introduce our novel general-purpose platform called TouchCom. In Section 4 we describe BCC infrastructure objects that can be built on top of the TouchCom hardware/software platform. The aim of this paper is to show that the BCC signal is strong enough throughout the whole body to be able to transfer data, even if at least one end of the communication is a mobile, standalone device. Therefore, in Section 5 we first validate that the signal is indeed propagates throughout the human body, then we test it in several setups including several users, various locations on the body, and different BCC objects. The application section (Section 6) demonstrates how the presented BCC infrastructure can be used for ubiquitous identification, tracking, or games. Finally, Section 7 concludes the results of the paper.

## 2 BACKGROUND

In this section we review directions on building smart infrastructure, as well as previous body channel communication work, with attention to projects that combined these two areas.

### 2.1 Smart environments

Ambient intelligence emphasizes the role of the environment in a ubiquitous computing. Such smart environments range from collaborative work [6], education [19, 29, 34], assistive living and fall detection [7, 12, 24, 33, 55], activity recognition [32, 60], and body posture detection [11, 20, 41] through dance floors [18, 31, 47, 56, 58], games [13, 38, 42, 44], and sport applications [26] to the concept of *everywhere internet* [16]. The underlying technology in these applications varies, depending on the objective of the system.

A crucial part of ambient intelligence is user identification and tracking whether it is a smart floor application, it is a reactive wall projection, or other interactive installation. This functionality can stand on its own for localization/positioning applications and can answer questions such as if the user is present at a certain location or not, which path did the user follow, who is standing where, etc. Tracking is often achieved by using computer vision with (mostly depth-)cameras [19, 29, 34, 42] or with visible light or infrared radiation [35, 58], wireless technologies (Bluetooth, RFID [22, 28]), pressure and force detection sensors [6, 11, 13, 24, 32, 33, 38, 41, 43, 44, 48, 56, 58], or capacitive sensing [12, 20, 26, 55, 59, 60].

Vision based solutions often suffer from constraints like occlusion, shadows (when installed in front) or heavy instrumentation (when installed in rear), ambient light, or high cost. BCC-based systems (e.g. a BCC-enabled floor) are not sensitive to lighting conditions, the modular design makes installation easy and does not require any high cost components. Radio-based wireless technologies do not provide whole-body range localization as they always show only the associated tag's position. In a BCC-based tracking system, the BCC device and the user's body together form one entity. Pressure and force detection sensors, as well as capacitive sensing, often lack user identification, but even if they support it, calibration and training is necessary. Consequently, these systems are severely limited in the number of users. Although BCC-based tracking requires user instrumentation, in return the positioning system is robust, accurate, and scales well (both in the number of participants and the size of the identifiers).

If the smart environment is already able to collect tracking information, the design can be extended by adding visual or other feedback, and the floor or wall can serve as an interactive surface. While most systems use front [4, 5, 31, 34, 42] or rear projection [11, 19, 29, 58] to achieve a high resolution or a wide area display, some of them use LED patterns [38] or strengthened LCD screens [13, 26] built into the floor. The presented BCC infrastructure introduces a floor system that provides visual feedback by incorporating 32 individually programmable RGB LEDs around each sensing location, resulting in 128 LEDs per floor tile ( $40 \times 40\text{cm}^2$  area). This display design results in a reasonable compromise between price, robustness, and resolution.

## 2.2 Body channel communication systems

The basic idea of BCC was first shown in [65, 66]: a modulated electric field was capacitively coupled to the human body, which then was able to relay information between the electric field source (transmitter) and the target (receiver). In these early setups no true wearable devices were demonstrated yet, nor was the system able to function standalone. While afterwards most work focused on the characterization of the human body channel [8, 9, 37, 50], different electrode placements [46], concepts of application scenarios [40, 45], advanced hardware design [15, 53, 54], or interaction with commodity devices [25, 27], only a few of them described interactions extended to the (BCC-enabled) infrastructure.

DiamondTouch represented a collaborative work environment with a real multiuser multitouch surface [14]. The user interface was projected from above onto a table that had special transmitters embedded into it. Each user sat on an instrumented chair with a built-in receiver. The table could uniquely identify which user was touching it and exactly where (based on the transmitter density of the desk). Another instrumented, but more lightweight desk was developed to demonstrate BCC for ubiquitous interactions and perception [21]. While these efforts opened discussions on how BCC could be used for ambient intelligence, the users were still limited in their location and movements.

Closest to our work is CarpetLAN [16], a smart floor system consisting of  $1 \times 1 m^2$  modules. CarpetLAN aimed to provide wireless-like networking in large areas using the users' body as connection between the Ethernet-floor and portable devices. The CarpetLAN tiles require a special electro-optic BCC transceiver component that raises cost, complexity, and power consumption. In contrast, the goal of our approach is to develop a low-complexity, lightweight system that encourages physical interactions. For these reasons, our devices use only off-the-shelf components. Our floor design provides  $20 \times 20 cm^2$  sensor resolution with visual feedback, does not require heavy cabling during interconnection, and instead of avoiding multiple participants to be in contact, we demonstrate applications that can leverage this scenario.

## 3 TOUCHCOM: A BODY CHANNEL COMMUNICATION PLATFORM

While laboratory setups can successfully demonstrate the basic ideas of BCC, they are not designed to be used as end-to-end systems: laboratory setups [8, 10, 30, 36, 37, 39, 51, 54, 63, 65, 66] are often evaluated only with additional devices attached that can unintentionally affect the signal level, making the measured data ambiguous (see Section 5); various setups [14, 25, 27, 39, 50, 57, 61, 63–66] are designed for a fixed, one-way communication that limits more advanced networking; some other setups use high-cost components [49, 53], do not present any form of user study or measurements [15, 40, 45], lack validating full-body range, wearable condition [9, 10, 23, 54], or miss adaptivity between changing signal levels during operation [46]. Since our goal is to provide technology that can be used efficiently in smart environments with as much freedom as possible, we present a novel, general-purpose BCC platform.

TouchCom is a lightweight, flexible and extendable BCC prototype platform. Most of the processing is pushed to the software side, minimizing the number of tasks (and parts) for the hardware and minimizing time spent in the analog domain. A software-focused approach has several additional benefits as well. Changing the system is faster and easier than is the case for a hardware-heavy system. Context awareness, adjusting parameters and configurations during operation, adaptivity across a wide range of conditions can be achieved. Furthermore, this architecture provides a suitable base for BCC networking, including (automatically coordinated) bidirectional data transfer, and successful communication across several concurrent participants.

The design parameters and constraints of TouchCom were derived from the intended use as an additional interaction technique for ubiquitous computing in modern intelligent environments: the instrumentation of the user should be minimal and as unobtrusive as possible; the system should support a wide range of different users;

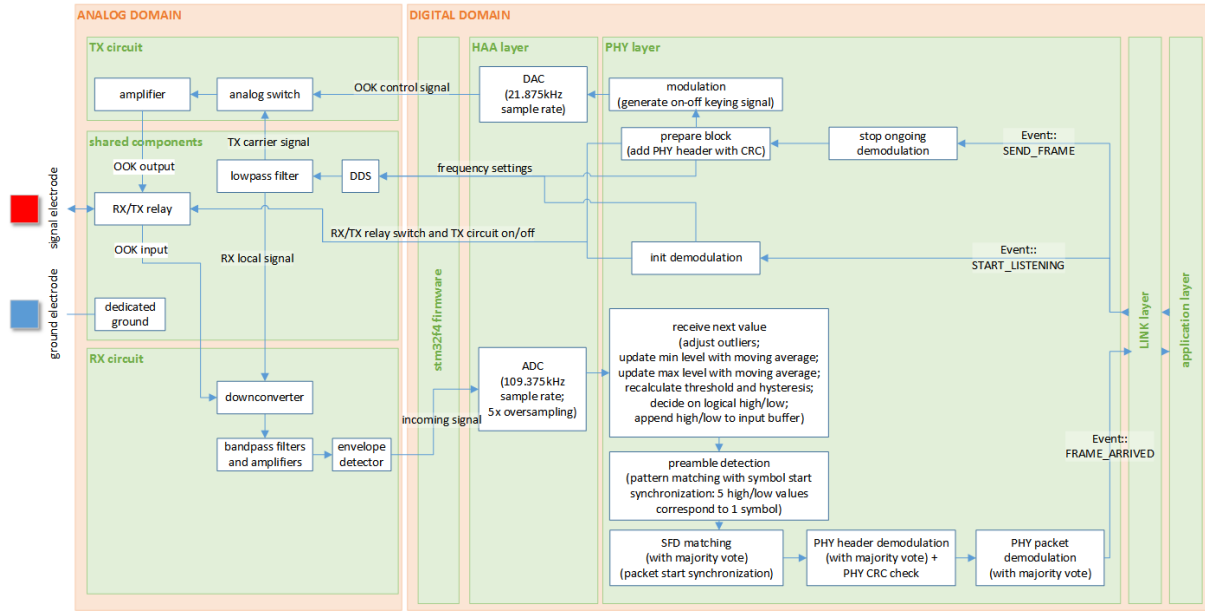


Fig. 2. High level overview of the TouchCom platform, focusing on the hardware/software codesign. Time spent in the analog domain is minimized. Details on the STM32F4 firmware, LINK layer, and application layer are omitted here for simplicity.

the contact points in the environment should be easily and conveniently accessible; over-the-air signal leakage should be minimal to avoid interference between concurrent participants.

These requirements can be more easily met by using the extrabody transmission through an electric field. (For a discussion of different techniques we refer to the appendix of this paper (Section A).) This approach does not require direct connection with the skin (transceivers can be separated from the human by a layer of clothes and can be placed in pockets, shoes, etc.) and scales better between various users (depends less on the body structure). As the size of the human body is of the same order as the wavelength corresponding to frequencies around 40 MHz, this range leads to unwanted radiation into the surroundings (antenna effect). However, there is no clear understanding on this radiation or near-field electrostatic air-coupling effect. Thus, we suggest to avoid high frequencies and focus on the lower range, which can be modeled by the *capacitive coupling* model (primarily the 1 MHz - 40 MHz range).

### 3.1 Hardware design

Some applications may require bidirectional communication (for example, whenever an acknowledgement must be sent back to the originator of a message, as is done in many protocols of the IP stack). A full-duplex design (when the transceiver is able to transmit and receive simultaneously), however, is a significant challenge. Following the capacitive coupling transmission model, there are two dedicated electrodes that connect each BCC device to the human (signal electrode) and to the environment (ground electrode). Having a full-duplex design would mean to have two signal electrodes: one for transmitting (TX) and one for receiving (RX). These electrodes, however, would need to be placed far away to prevent the RX to overhear its own TX signals. This placement would cause heavier instrumentation and would degrade the user experience. Thus, BCC devices should be designed to operate as half-duplex devices when bidirectionality is needed (the transceiver is able to transmit

and to receive, but cannot do both at the same time) [65]. The TouchCom board has both TX and RX capabilities and can be switched between these two modes by software. Figure 4a shows the realized TouchCom half-duplex transceiver (TRX) PCB. For a high level overview of the hardware-software system, we refer to Figure 2.

The TX part of the hardware is responsible to provide a modulated signal with the desired frequency and amplitude. Since the users are capacitively coupled to the BCC device through the dedicated signal electrode, the system naturally acts as a high pass filter. Even though there are examples using wideband modulation for BCC (e.g., by applying baseband square signals directly) [15, 23, 49, 53, 54], these systems are more susceptible to noise in the (unregulated) frequency range in question. Therefore, the applicability of these solutions for wearable, full-body range scenarios needs further investigations.

Our implementation uses narrowband OOK (on-off keying) modulation, with a high frequency carrier signal. The carrier is generated by an AD9851 DDS (Direct Digital Synthesizer), which can be set to an arbitrary frequency in a wide range. During the evaluation described in this paper, 8 MHz was used (except when indicated otherwise). This frequency falls into the target frequency domain we described earlier, and previous studies also indicated that this is a well performing option [3, 8, 37, 50]. The discretized sinewave generated by the DDS is filtered by a lowpass filter to suppress harmonics. The OOK modulation is achieved using a MAX4544 analog switch. The baseband signal for the 21.875 kHz OOK modulation is generated by software. This control signal switches on and off the carrier frequency, resulting in an OOK modulated signal. The modulated signal is fed into a 3-stage amplifier achieving at most 10 V peak-to-peak output signal level. (At 2, 3, 4, and 8 MHz carrier frequency the output voltage is 5.9, 8.6, 9.9, and 6.1 V peak-to-peak.)

In the RX part the aforementioned DDS and the lowpass filter are utilized to generate the local signal. An SA602 four-quadrant multiplier is used to downconvert the signal intercepted on the RX electrode pair. This IC has a relatively high ( $1500\ \Omega$ ) input impedance, which is advantageous as the input stage of the BCC system. The downconverted signal is then filtered and amplified by a two-stage bandpass filter and amplifier IF (Intermediate Frequency) system. The bandwidth of the filters are set to 200 kHz. The envelope of the signal is detected by a MAX9933 logarithmic level detector which is then fed into the ADC unit of the microcontroller.

Designing the hardware to be half-duplex required special considerations. First the signal must be routed between the receiver or the transmitter and the electrodes. The TX/RX switching is accomplished by a bistable relay, which provides low leakage even for impedances far from the ideal 50 Ohm. To save energy and to prevent the possible interference between the TX and RX side, the power supply of the transmitter amplifiers must be turned off with an electronic power switch when they are unused.

### 3.2 Software architecture

The prototype is equipped with a removable Mini-M4 STM32F415RG microcontroller to ensure convenient access during development. As opposed to earlier work, we put emphasis on building a flexible, modular, but maintainable software platform. The architecture consists of several layers to separate responsibilities and to support decoupling (separation between software modules). The layers build on top of each other as follows: 1) microcontroller firmware (third-party, distributed by the libopencm3 community [2]); 2) HAA (hardware abstraction architecture) layer as a bridge between hardware dependent and independent code; 3) PHY (physical) layer to perform data encoding and modulation; 4) an optional LINK layer to coordinate sessions between several communicating devices; and 5) higher-level application code. In the following paragraphs we provide details on the physical and link layer implementation.

**3.2.1 Physical layer.** Each message starts with three preamble bytes (0b10101010), followed by a start frame delimiter (SFD, 0b10101011), followed by the PHY packet (see Figure 3). The size of the PHY payload can be varied between 0-252 bytes and is described in the PHY header (which is 3 bytes itself). The purpose of using that specific preamble pattern and repeat is to allow enough time for the RX to lock on the right timing (symbol

start synchronization), while the SFD is used for packet start synchronization. The message size is limited since the oscillators dictating the TX transmission and RX receiving can slightly drift with time, resulting in errors even when working with devices that are initially synchronized.

The PHY layer takes the digital information to be transmitted, prepends a PHY header and then generates the bitstream of whole message for the OOK modulation. The TX code results in a 21.875 kHz frequency OOK control signal. This signal appears as the output of a 12-bit digital-to-analog converter (DAC). The RX microcontroller sample frequency is 109.375 kHz, and it uses a 12-bit analog-to-digital converter (ADC). With this setup, 5 sampled values describe one symbol (bit) of the original message. This oversampling allows basic digital filtering by using majority vote to decode each message bit.

The RX must be able to adapt to different signal levels: weaker or stronger connections vary based on the quality of the capacitive coupling. To meet that requirement, adaptive thresholding is used in the program: the expected high and low signal levels adapt according to the minimum and maximum values seen in the past using moving averages. Thresholding as well as preamble detection and decoding all happen in the PHY layer. As soon as one preamble pattern is recognized, the demodulation algorithm decodes the next byte. If that byte is not a preamble or SFD, then it is dropped, and the algorithm restarts looking for a preamble. If the byte matches the SFD, then the system continues decoding the PHY header. The third byte of the PHY header contains a cyclic redundancy code (CRC) to ensure that the important parameters (like size) correctly arrived. If the CRC is corrupted, or the decoded size is 0, then the packet is dropped. Otherwise, the message is decoded and handed over to higher software layers.

**3.2.2 Link layer.** The chosen OOK modulation cannot prevent occurrence of collisions of concurrent messages over the same channel. To allow multiple users to participate at the same time without collisions, two different link layer approaches are implemented for medium access control (MAC): Random Waittime Beacons (RWB) and Aloha. In the case of RWB, all transmitters send their messages continuously, but they wait a random time between transmissions. If there are only a small number of devices, this setup is efficient enough to ensure a high probability of transmitting at least one successful message from each transmitter in every second - resulting in a still adequate response time of the system, while it avoids the overhead of a more advanced MAC. Aloha is a more sophisticated option that is implemented together with a sliding window protocol as logical link layer; each TX sends a message whenever it is requested by its upper layers.

### 3.3 Safety

In BCC systems, safety and health concerns must be carefully addressed. The occurring effects are highly dependent on the frequency and the amplitude of the current. For the presented capacitively coupled system, we follow the guidelines on *Limiting Exposure to Time-Varying Electric, Magnetic and Electromagnetic Fields (Up to 300 GHz)* issued by ICNIRP [1]. In the 8 MHz domain, basic restrictions are provided on current density, to prevent effects on nervous system functions, and on SAR (specific energy absorption rate), to prevent whole-body heat stress and excessive localized tissue heating. The maximum contact current of the system is less than 0.5 mA subject to the safety limit of 20 mA. The whole-body average SAR is less than 1 mW/kg subject to the safety limit of 80 mW/kg.

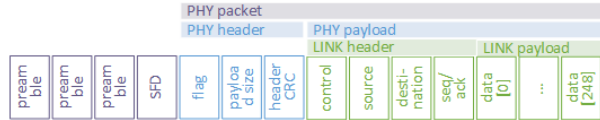


Fig. 3. Frame structure.

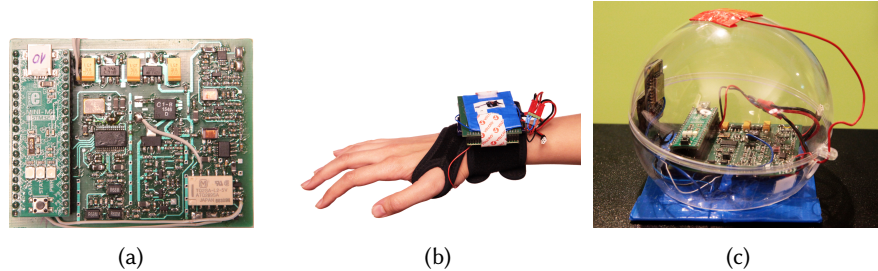


Fig. 4. (a) TouchCom transceiver PCB (size approx.  $7 \times 7\text{cm}^2$ ). The signal and ground electrodes connected to the PCB are made of copper tape. Since capacitive coupling is used, direct (galvanic) contact to the skin is not required, therefore the electrodes are insulated; (b) Mobile BCC wearable (wristband): the signal electrode is insulated by red and the ground electrode by blue tape; (c) Portable BCC terminal (sphere): the touch point is indicated by a red tape. The diameter of the sphere is 10 cm.

#### 4 DESIGN OF BCC INFRASTRUCTURE

The presented system leverages the advantages of body channel communication and provides a platform to create a human-centered ambient intelligence. A BCC-enhanced smart infrastructure can robustly provide user identification and tracking information, while enabling an engaging form of communication and interaction: it enables whole-body range activated interactions, and gives the control to the user to establish and conduct communication between different objects and devices. We present three different prototypes for a BCC infrastructure as shown in Figure 4 and 5: BCC wearables, portable BCC terminals, and BCC floor/wall tiles; they are all based on the core TouchCom transceiver PCB.

##### 4.1 BCC wearable (wristband)

The important difference between embedding BCC into mobile devices or into the environment is the grounding: while fixed installations have much stronger connection to the earth ground, wearables only have parasitic capacitive coupling through the air. Consequently, wearable versions have much weaker and noisier signals. The TouchCom prototype boards are designed and tested in such a way that they are suitable to be used in these wristbands (Figure 4b). A 7.4 V battery is needed for operation.

##### 4.2 BCC terminal (sphere)

A BCC terminal with a sphere shape is designed with the purpose of being easily accessible by several users at the same time (see Figure 4c): the participants can stack their hands on top of each other while only the bottom one touches the sphere directly. The same TouchCom prototype transceiver can be found inside the sphere as in the case of the wristband. The BCC terminal is portable and can be placed on any desk or the floor; it is powered by a 7.4 V battery. The sphere is equipped with an LED strip to provide fast, direct visual feedback but can be connected to external displays as well.

##### 4.3 BCC floor/wall tile

The BCC-enabled (floor/wall) tile exploits the key idea of BCC: the signal that flows through the human can be detected at any point of the body, including the feet or hands. Multiple instances of these tiles are then connected to cover the floor or a wall (of a room). The idea is that the users wearing the wristband can walk on the floor or touch the wall while each tile can identify who is standing on it or touching it.

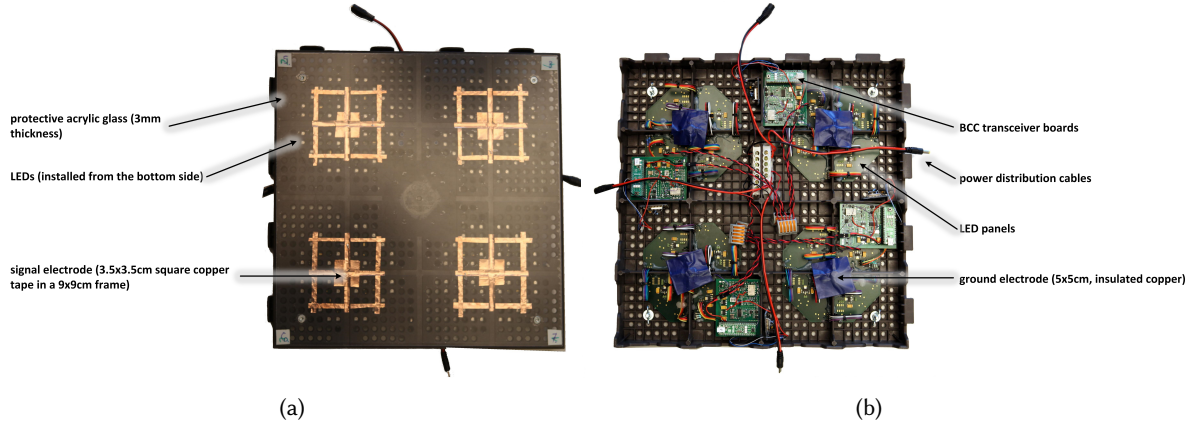


Fig. 5. BCC floor/wall tile design. (a) Top view of the tile with LEDs (size  $40 \times 40 \text{ cm}^2$ ); (b) Bottom view with transceiver boards.

As a base, we use  $40 \times 40 \text{ cm}^2$  outdoor plastic floor tiles that are readily available at building supply stores. Multiple tiles are connected to form a demonstrator system. These tiles are robust enough to sustain walking and jumping, yet they are lightweight (1.4 kg/tile). We instrument each floor tile with 4 signal electrodes ( $5 \times 5 \text{ cm}^2$  each, copper) in a square shape in the middle of the tile, as seen on Figure 5a. We place the ground electrodes at the bottom of the tiles. This setup results in a  $20 \times 20 \text{ cm}^2$  resolution for user localization. On top of the electrodes we add a thin acrylic glass protection layer. This kind of insulation is possible because TouchCom builds on capacitive coupling, which does not require direct galvanic contact. The bottom part of the tile can accommodate all the necessary electronics (Figure 5b): each electrode pair is connected to one BCC prototype transceiver board. To provide visual feedback, we added 32 LEDs placed around each sensing location. These LEDs can be programmed individually and can light up in any RGB color.

#### 4.4 Power supply

In a capacitively coupled system grounding is an important factor. A direct ground connection (galvanic connection to the building power supply system) can boost signal levels. If a system is designed and only evaluated using direct grounding, the performance of the portable (battery powered) versions may drop below usability thresholds.

While the presented wearables and terminals are primarily used from battery, the tile design is tested also when powered from the building's power system. Battery-based operation enables portability and provides full galvanic separation between the sensors; on the other hand, a larger area is more conveniently powered up and controlled using the building's outlets. The power supply unit (PSU) can be optionally connected to the system. During evaluation we used a 12V, 480W switch mode PSU connected to one of the building's power outlet. It can provide a stable power source for at least 16 floor tiles. The PSU, however, does establish a galvanic connection between the four sensors of a tile (and between any additional tiles as well) through the shared ground. Section 5.7.4 discusses the performance difference between usage in both power supply cases.

It is important to note that in each case, the circuitries of the LEDs are isolated from the transceivers and the microcontrollers with optocouplers to reduce the possible interference. In the battery operation mode they use a separate battery. When operated from the PSU, the whole tile uses the same power supply, but the spikes on the voltage rails generated by the LEDs are much smaller.

#### 4.5 Connectivity

As today's SoCs provide ample processing capabilities, we provide an optional WiFi feature for each BCC prototype; this functionality allows us to connect each device easily to already existing backbone systems and simplifies debugging, error logging, and performance measurements.

### 5 EVALUATION

We evaluate the BCC objects in several dimensions to understand the limits of the overall system, while validating the design goals as described earlier (see Section 3): *the instrumentation of the user should be minimal and as unobtrusive as possible; BCC should support a wide range of different users; the contact points in the environment should be easily and conveniently accessible; over-the-air signal leakage should be minimal to avoid interference between concurrent participants.*

Setting up a suitable measurement system to allow evaluation of BCC wearables poses some challenges. If any of the devices is connected to the earth ground, then the entire system will be short-circuited to that ground immediately. This connection results in a signal path that is much stronger than the path of the original design (when coupled only through the environment), leading to erroneously increased detections of transmissions. Although this might seem a desirable side effect, this setup does not correspond to mobile application scenarios and therefore would lead to misleading conclusions.

To allow a realistic setting, we evaluate the BCC transmissions using measurements from the hardware prototypes themselves, instead of using separate measurement hardware (like a handheld oscilloscope). There are several reasons for this approach. First, we can make sure that the prototype design is suitable to operate as wearable when only parasitic ground coupling is available. Second, we can measure the properties of the transmission of a real, modulated signal, not just measuring an unmodulated carrier. Third, we can validate the performance of the analog circuit.

Gender	5 female, 10 male		
Age	22	-	38
Weight (kg)	50	-	106
Height (cm)	165	-	190
Shoe type	running shoes, canvas shoes, outdoor shoes, leather shoes, high heels		

Table 1. Pool of participants for preliminary evaluation of the system. The different body parameters have an impact on parasitic over-the-air signal leakage; the shoe type influences the leakage to the ground.

In the following we describe several measurement setups. Even though a comprehensive user study is outside of the scope of this paper, we present the results as an indication that the BCC system can perform well across different users. Various users participated in the evaluation interacting with each other, with the terminal, and with the tiles. A summary of all the users participating in at least one evaluation can be seen in Table 1.

#### 5.1 Metrics

We present signal to noise ratio (SNR) values as indicators of signal strength, establishing a comparable metric for the different setups. These values are crucial to understand the possibilities and to show usability for whole-body scale use cases.

Traditional SNR calculation is defined as the ratio of the power of a signal ( $P_{signal}$ ) and the power of background noise ( $P_{noise}$ ). In the case of the chosen OOK modulation, the logical low values correspond to the noise level, therefore the SNR value can be calculated as the ratio of the signal level of the logical high values ( $P_H$ ) and the signal level of the logical low values ( $P_L$ ). This value equals to the difference of them if the signals are given in

dBm ( $P'_H$  and  $P'_L$ )), as well as the difference of them if they are given in dBmV ( $V'_H$  and  $V'_L$ ).

$$SNR = 10 \times \log_{10} \frac{P_{signal}}{P_{noise}} = 10 \times \log_{10} \frac{P_H}{P_L} = P'_H - P'_L = V'_H - V'_L \quad [dB] \quad (1)$$

To calculate the SNR on the microcontroller, the recorded ADC values have to be used. The ADC values range between 0 and 4095, with corresponding input voltage of 0 to 3.3 V. However, the signal detected at this point has already gone through analog processing and does not correspond to the input signal as is detected at the signal electrode of the RX; the MAX9933 logarithmic level detector in the analog RX chain already provides the dB-proportional signal level (with sensitivity of 27 mV/dB), therefore the signal sampled by the ADC does not need logarithmic transformation.

However, the RX chain also contains nonlinearities. Therefore, the voltage level measured after the detector (and consequently the ADC values) do not directly reflect on the power of the incoming signal (at the entry point of the RX, i.e., at the signal electrode) and cannot be used “as is” to calculate the SNR. To derive the actual signal levels (and SNR) from the ADC values, the connection between the real input voltage at the signal electrode of the RX and the voltage as measured by the ADC must be formalized. To derive this function, we supplied the input of the receiver with the (known) signal of the transmitter through a variable attenuator and measured the detected signal level on the ADC. We recorded the ADC level for multiple different input signal levels and then approximated the response curve with functional fitting using a 3-parameter logarithmic function (see Figure 6) and obtained the following formula:

$$V' = 7.304 \cdot \ln(V - 306.72) + 9.95 \quad [dBmV] \quad (2)$$

where  $V'$  is the voltage level at the signal electrode of the RX, and  $V$  is the voltage level at the microcontroller:

$$V = \frac{ADC}{4095} \cdot 3300 \quad [mV] \quad (3)$$

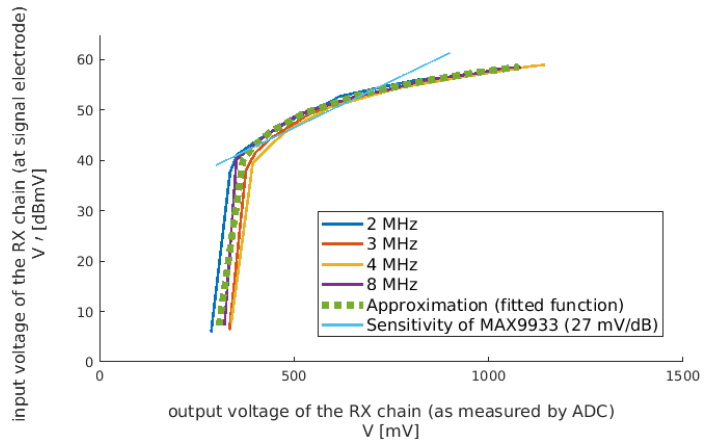
Therefore, SNR can be calculated from the ADC values using the combination of Equations 1, 2, and 3:

$$SNR = (7.304 \cdot \ln(\frac{ADC_H}{4095} \cdot 3300 - 306.72) + 9.95) - (7.304 \cdot \ln(\frac{ADC_L}{4095} \cdot 3300 - 306.72) + 9.95) \quad [dB] \quad (4)$$

$$SNR = 7.304 \cdot \ln\left(\frac{\frac{ADC_H}{4095} \cdot 3300 - 306.72}{\frac{ADC_L}{4095} \cdot 3300 - 306.72}\right) = 7.304 \cdot \ln\left(\frac{ADC_H - 380.612}{ADC_L - 380.612}\right) \quad [dB] \quad (5)$$

where  $ADC_H$  and  $ADC_L$  are the corresponding average ADC values for the input voltage (after the RX detector) of every received high and low values (of the received and demodulated packets).

Fig. 6. The relationship between the voltage level at the end of the RX chain and the beginning of the RX chain.



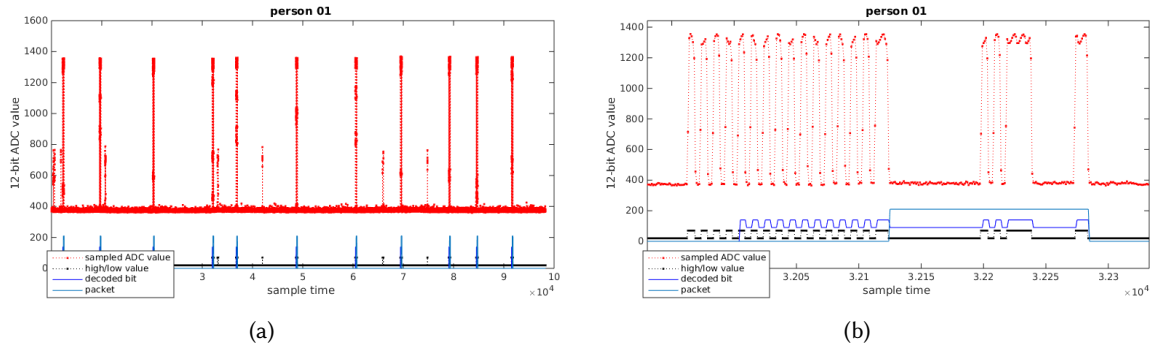


Fig. 7. (a) Person 1 touches the sphere with his/her instrumented hand. Rising signal levels are present at various times. The data shows 98304 sampled values, in total a 0.9 s measurement window length.. The small spikes are noise coming from the WiFi module; (b) 4 ms enlarged window of (a), showing the packet at  $3.2 \times 10^{-4}$  s.

Only after understanding the physical limits of the BCC transmission (e.g., indicated by SNR) can one move forward to the application level and evaluate the setup as an end-to-end communication system using traditional network metrics. While the main goal of this paper remains to present practical, standalone end-user BCC enhanced objects that indeed use the body as transmission medium across its whole dimension, we also provide data rate, packet error rate (PER) and bit error rate (BER) values for several setups. While the SNR values reflect on the hardware sensitivity, data rate and PER are mostly tied to the performance of the current software implementation. Therefore, the SNR values are a good indicator of the possibilities enabled by the TouchCom platform.

## 5.2 Signal strength measurements

We perform measurements with TouchCom boards where a dedicated TX is configured for continuous transmission with an 8 MHz carrier (unless indicated otherwise). The measurements on the RXs are triggered through WiFi to synchronize the different sensors (when measuring with several sensors simultaneously), to ease data collection, and to maintain galvanic separation. Each measurement window is limited to approx. 300ms due to limited storage space in the microcontroller. With a sample rate of 109.375kHz, one window includes 32768 ADC values. Each measurement is repeated three times with approx. 2-3 min time difference between them. The TX send times are not synchronized across the measurements, therefore the recorded signals are not comparable directly in the time domain. For the presented statistics below, the average values are used from the repeated measurements.

The firmware code of the RX is ported to a simulation environment for a detailed offline analysis of the data and the RX behavior. Figure 7a shows a full measurement session. For easier depiction the 3 repeated measurements are concatenated on the plot to a 0.9s window. The graph shows in red the measured signal value (i.e., ADC output, left Y axis, ranging between 366 and 1354). The bottom part shows in blue which value was decoded (right Y axis) and if a packet is being processed. Figure 7b shows a detailed view of a single packet – a clear signal is observed and the packet can be decoded.

Since the input signal strength can vary significantly, the RX software is prepared to adapt. Using the simulation we can clearly see how the RX decides to categorize certain input values as logical high or low (black line). After that decision the demodulation code tries to match a preamble. If that happens (rising edge of the dark blue line), the system starts decoding the data bits (dark blue line). Once the SFD byte is successfully found, the RX proceeds with decoding a packet (light blue line).

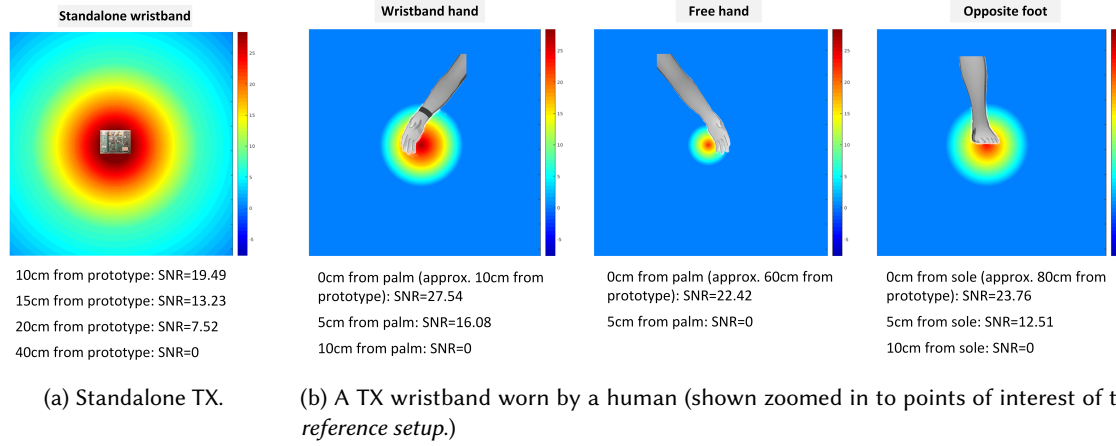


Fig. 9. Signal propagation around a human and on over-the-air signal leakage. Two setups are evaluated: Figure 9a shows the signal strength around a standalone TX (configured for continuous transmission); Figure 9b shows the signal around a (continuously transmitting) wristband-wearing human. The signal strength is measured with a separate receiver (placed on a desk/floor) at several distances (0-40 cm) in one dimension. For simplicity and comparability of the order of magnitude, 2D heatmaps are shown (considering only the effects originating from the contact point, not including surroundings, i.e. other body parts).

### 5.3 Signal propagation

The principle of BCC is that human presence is needed for successful communication between BCC objects. However, the quasi-static near-field coupling does not only couple the BCC device to the body that it is in direct contact with, but it occurs for some distance over the air as well. As the exact behavior has not been published in prior work, we present here empirical data to prove that the human body indeed is crucial to extend the signal's reach. At the same time we show the magnitude of the over-the-air signal leakage.

For these measurements an 8 MHz carrier was used. Figure 9 shows two different setups. First, we measure air-coupling around a transmitting wristband. In this setup, no human is present. The heatmap shown on Figure 9a is based on the SNR values that are measured at air distances of 10, 15, 20, and 40 cm between the TX and RX devices. Figure 9b presents the SNR values that are measured around the human (see Figure 8), while the person is wearing a transmitting wristband. These heatmaps show direct touch on the dedicated point, then 5 cm, and finally 10 cm further away from the point.

The measurements prove that the human body significantly extends the signal's path: without the human the signal drops below the detectability threshold by 40 cm; however, it is detectable with high SNR (above 20 dB) at far locations of the body (60-80 cm from the wristband). However, some over-the-air coupling occurs as well: it is stronger around the TX (up to approx. 10-20 cm) and weaker everywhere else (up to approx. 5-10 cm).

### 5.4 Relationship between signal strength and throughput

As an indication of the current overall system performance, we present throughput, packet error rate (PER) and bit error rate (BER) values. The baseband modulation is 21.875 kHz, consequently the best achievable

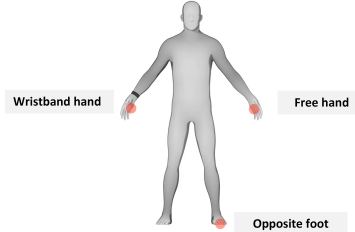


Fig. 8. Reference setup.

bit rate is 21.875 kb/s. However, there is some communication overhead in the system caused by the preambles and the SFD. Therefore, when calculating the throughput these bytes are not included in the number of successfully decoded bytes. While the throughput is calculated by measuring successfully decoded versus lost or damaged packets, PER shows the percentage of the packets that arrived completely correct, and BER shows the percentage of the correctly arrived bits (also including valid bits from corrupted packets).

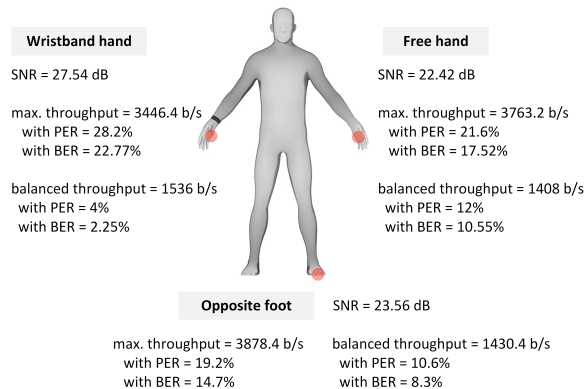


Fig. 10. Throughput, PER, and BER based on the *reference setup* (three measurement locations, while the user is wearing a continuously transmitting wristband). Send intervals are 30 ms for a balanced throughput/PER rate, and 10 ms for maximal throughput.

on the signal strength. While we present only SNR values for these setups, we refer to this current section as reference to indicate the relationship between SNR and achievable PER/BER/data rate performance.

## 5.5 BCC wearables

The BCC system is further evaluated regarding portability with the handshake scenario, originally proposed by [66]. However, instead of placing the prototypes 'near the feet' [66], wearable wristbands are provided to the users, creating a more realistic scenario. The measurements are performed by two users randomly selected from the user base. One of them has a wristband that continuously transmits an ID every 200 ms. The other participant has a wristband programmed to receiving mode. As described in the section on measurement methods, a  $3 \times 300$  ms measurement window is recorded. All possible combinations of the handshakes are tested by using each user's instrumented hand as well as using their free hand. The SNR values derived from the data collected during the measurements are depicted in Figure 11. As we can see from these values, having a wearable as receiver results in a similar signal strength as obtained for the wristband-free transmitter and (semi-)fixed receiver pair. This observation validates that TouchCom is suitable for wearables.

## 5.6 Multiple participants with a BCC terminal

The sphere-related experiments focus on the two main design goals. First, the terminal should work reasonably well for different users carrying the BCC wristband: the sphere should work whether the users touch it with

During these measurements 10-byte long messages are sent (3 byte PHY payload) in 100 packet bursts. Each measurement is repeated 5 times, and the average values are plotted. We measure the throughput around three dedicated points on the user following the *reference setup*. Figure 10 shows the system performance alongside with the signal strength measured in Section 5.3. The measurements prove that the same, stable throughput can be achieved throughout the whole body: the values are similar when measured at the palm of the wristband hand, at the palm of the free hand, and at the bottom of the feet as well. The data also show that reliable communication can be achieved at a rate of approx. 1.5 kb/s (with approx. 8% PER). If the application only requires beaconing (packets may get lost), the throughput can go up to approx. 3.7 kb/s. Beaconing (especially with short send time intervals like 10 ms) can be quite useful for tracking or other applications that rely on user identification.

In the following sections we present several configurations and evaluate the effect of several parameters

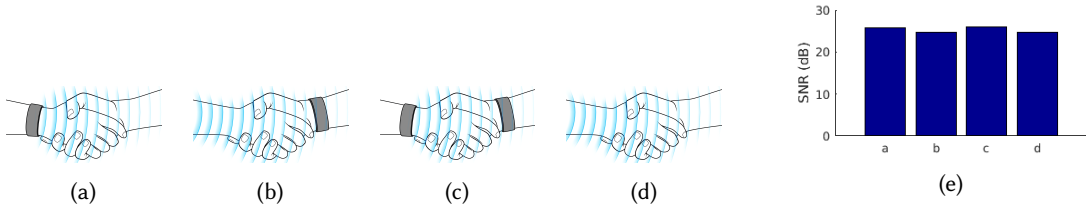


Fig. 11. Handshake scenario in all possible setups. 11a: person-TX has the wristband on the handshaking-hand, person-RX has the wristband on the hand not shown; 11b: person-TX has the wristband on the hand not shown, while person-RX has the wristband on the handshaking-hand; 11c: both participants use their wristband hands to handshake; 11d: both participants use their wristband-free hands to handshake; 11e: SNR values for all the setups (25.83, 24.68, 26.11, 24.78).

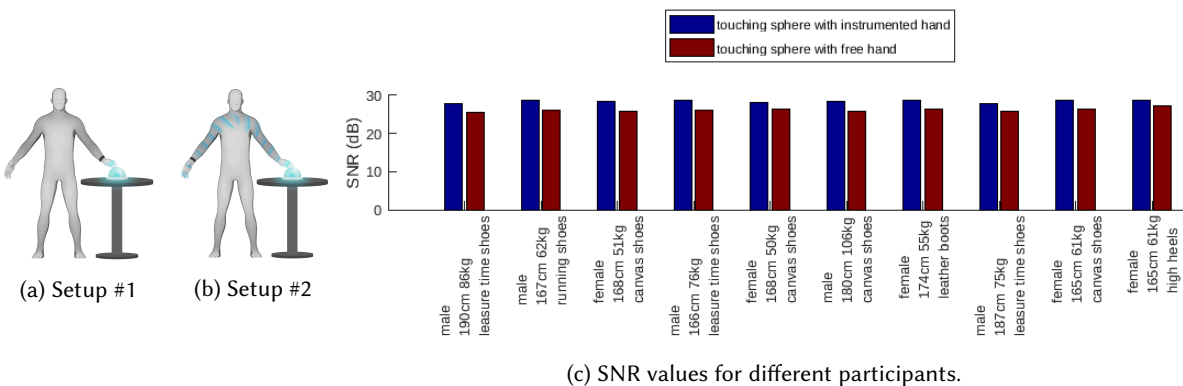


Fig. 12. Measurements performed by ten single user from the user pool. The participants have different body shapes and footwear. In each test one user touches the BCC sphere with her/his BCC wristband wearing (Setup #1) or her/his free hand (Setup #2). The SNR reflects on the measured signal strength at the sphere.

the instrumented or with their free hands. Second, the terminal should be able to recognize all the users when touched by several of them at the same time.

To evaluate individual differences between participants, each user is asked to touch the sphere while wearing one dedicated wristband: first with the hand that has the wristband, and then with their free hand. Figure 12a and Figure 12b show the experimental setups, while Figure 12 shows the corresponding SNR for each participant. The signal levels differ for each participant, and they decrease when the users touch the sphere with their free hand. However, according to the in-depth investigation using the simulation, the software is able to adapt to these changes and to decode the data successfully.

After the individual measurements, a group setup is considered. Three participants are asked to touch the sphere together: first with their instrumented hands and then with their free hands (Figure 13). Their wristbands are configured for continuous transmission, using the RWB protocol. The signal level clearly drops if touched by free hands compared to the sphere touched by the instrumented hands. This phenomenon is already noticeable by the individual measurements. However, there are two other aspects that make this measurement setup interesting. First, the random beaconing approach of the TX transmission is visible. The simulation code validated that in the measured  $3 \times 300\text{ ms}$  period, no collisions happened, and each participant's ID was detectable several

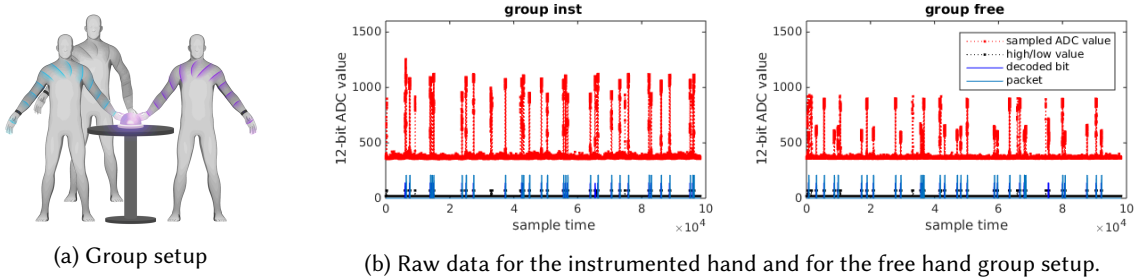


Fig. 13. Multi-participant scenario: person 2 & 3 & 4 touch the sphere at the same time. In one case they all use their instrumented hands, then their free hands.

times. Second, the measurement and simulation also show that the RX succeeds to adapt to different signal levels immediately (the ADC value for the logical high is significantly different for the different users).

### 5.7 BCC floor and BCC wearables

The following measurements are performed with one dedicated BCC tile and a dedicated wearable. The user stands on the same subtitle during the measurements, wearing a (battery powered) wristband. The tiles are powered by a PSU except when indicated otherwise.

**5.7.1 Wearable to floor unit.** Figure 14 shows the wristband sending data towards a floor tile. The figure depicts the tile in different setups. The first row shows measurements recorded wearing shoes, while the second row was recorded without them. The different columns show different carrier frequencies (in the limit range of the TouchCom transceiver: 2 MHz, 3 MHz, 4 MHz, and 8 MHz). The wristband is programmed to transmit one packet every 100 ms, while all four cells of the tile are receiving. The recorded data shows that a higher carrier frequency provides stronger signals, although at 8 MHz the signal also radiates to neighboring subtiles. Moreover, better contact to the signal electrodes (e.g., standing on the floor without shoes) also results in a stronger connection. However, even with shoes, the system can successfully send messages.

**5.7.2 Floor unit to wearable.** Figure 15 presents results for communication in the opposite direction: a floor unit attempts to send data towards a user's wristband. The measurement scenarios are identical to the ones described in Section 5.7.1, with the exception that the wearable receives and the subtitle on which the user stands transmits. Several conclusions can be drawn from this experiment. First, the signal levels on the two dedicated endpoints behave similar to the case when the receiver is directly grounded (as part of the PSU-powered floor) and the transmitter is battery powered: they have the same absolute value, and they change the same way as the frequency is varied. One may expect weaker signals if the receiver is battery powered since its ground is floating. However, the data indicate that to boost connectivity it is enough already if one endpoint has a direct ground connection. The second conclusion is confirming the electrostatic coupling behavior that was observed in Section 5.3: significant amount of signal leakage can be observed in the neighboring subtiles if the signal originates from a floor tile.

**5.7.3 Variance between users.** Similar to the hand-touch measurement as discussed in Section 5.6, participants are asked to stand on a dedicated tile while wearing a dedicated wristband. Even though the participants had different body types, clothing, and shoes, the measured signal strength indicates that communication is possible in both directions for each user in the set. Figure 16 presents the SNR for each individual participant setup alongside with their body parameters and shoe types.

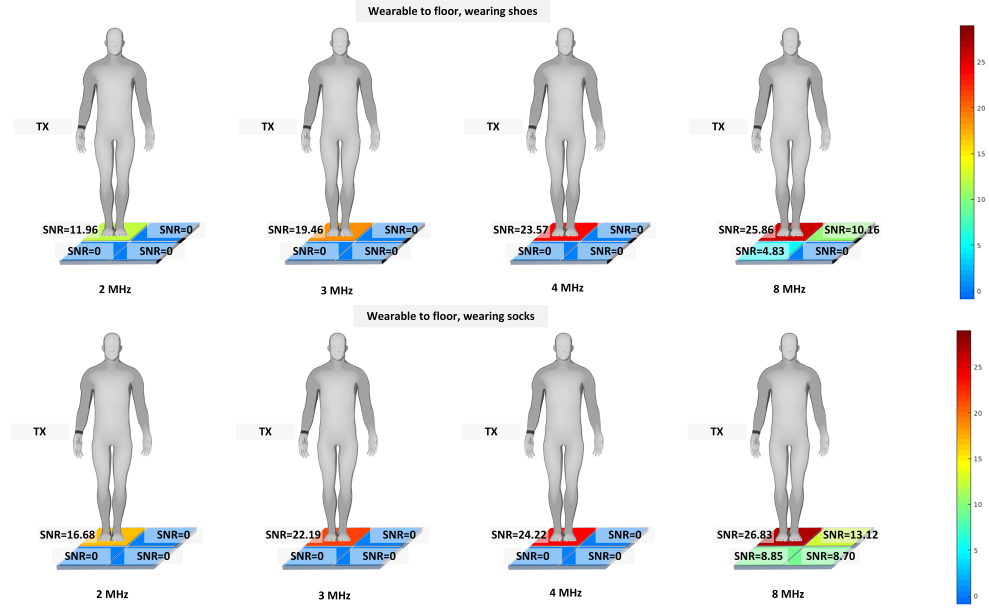


Fig. 14. Sending data from the wearable to the floor tile. The upper figure shows measurements performed while wearing shoes, while the bottom is measured while wearing only socks.

**5.7.4 Performance difference based on power supply.** Figure 17 shows how a BCC tile performs while operated from battery. When compared to Figures 14 and 15, it can be observed that the signal strength is slightly below the one measured while operated from the PSU. This outcome is expected since in the PSU-version the grounds are not floating. However, since the tiles have dedicated ground electrodes that are placed directly on the floor, the system performs well even without this explicit ground connection. Therefore, the observed signal levels are similar in both the PSU and the battery case. Additionally, the signal leakage (especially when the tile is transmitting) is lower when powered from a battery. The reason is probably not just the difference in grounding but also that each BCC sensor is using separate batteries, therefore there is no galvanic connection between neighboring tiles.

## 5.8 BCC floor without user instrumentation

In this paper we discuss the design of an enabling interactive infrastructure. If we want to keep the barrier of using this system as low as possible, then we want to explore a truly human-centered environment that works without instrumenting the users. Therefore, in addition to instrumented usage scenarios discussed above, we present here results for setups without the explicit need to wear any devices: users may simply enter into a BCC-enabled infrastructure and start to interact with it right away.

**5.8.1 Connecting BCC sphere to BCC tile.** Figure 18 shows that it is possible to send data not only between wristbands and tiles but also between tiles and portable terminals. Moreover, the SNR values indicate significantly stronger signal levels in all setups compared to the wristband-tile measurements. The higher gain probably can be explained by properties of the platform design: in the case of the sphere, the signal and ground electrodes are well-separated (approx. 10 cm vertically), whereas these electrodes are spaced much more closely on the wristband. There, the distance is at most approx. 5 cm, and this placement could lead to some leakage of the

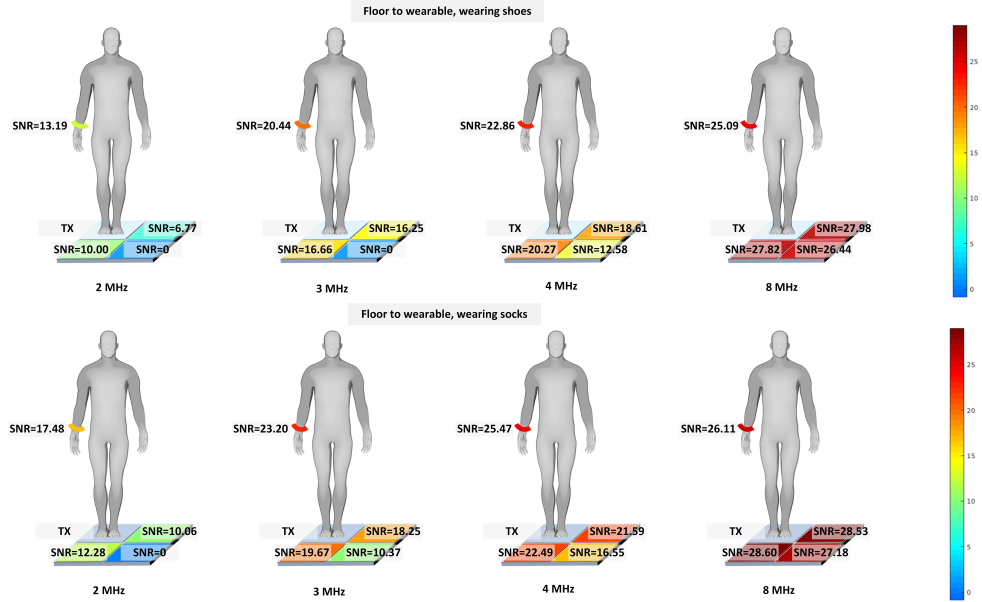


Fig. 15. Sending data from the floor tile to the wearable. The upper figure shows measurements perform while wearing shoes, while the bottom is measured while wearing only socks.

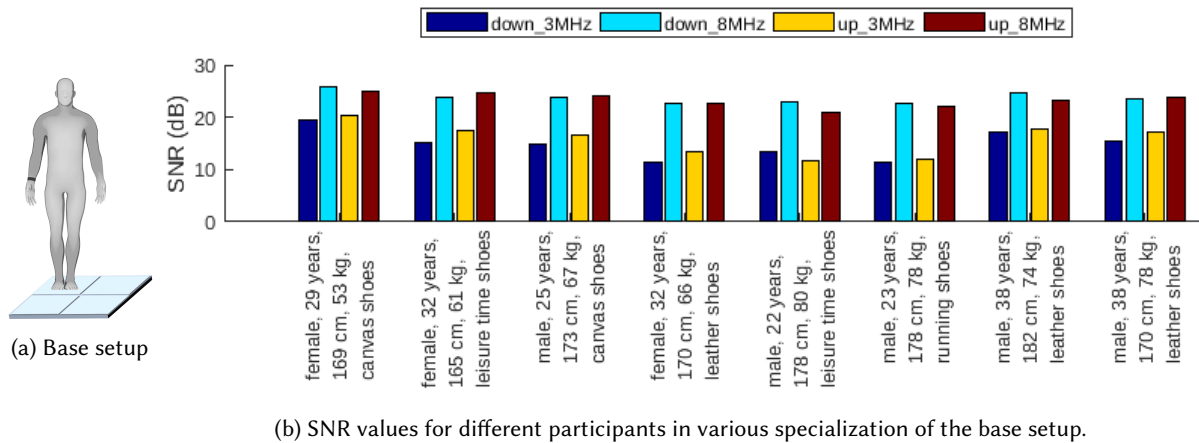


Fig. 16. Measurements performed by eight single user from the user pool. The participants have different body shapes and footwear. In each test one user stands on a BCC tile while wearing a BCC wristband. The different colors show the different setups: direction of the communication and the applied carrier frequency.

signal. During the measurements, the user stands on a PSU-powered tile while touching the battery-powered sphere. The sphere is placed next to the tile on a wooden table of height 110 cm.

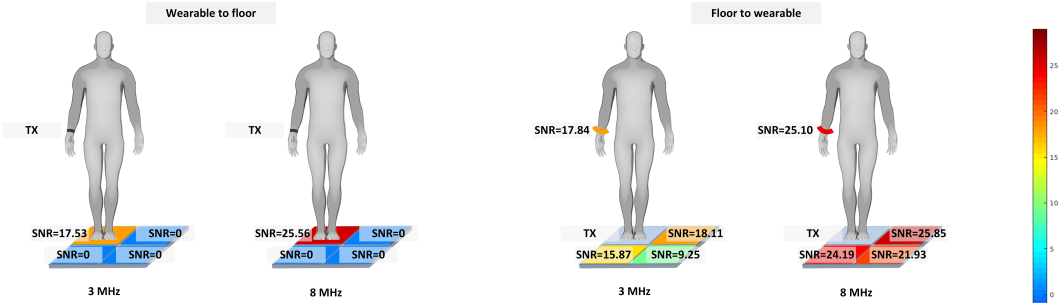


Fig. 17. Battery powered BCC tile: both data transfer direction is evaluated on 3 MHz and on 8 MHz as well. The user is wearing shoes.

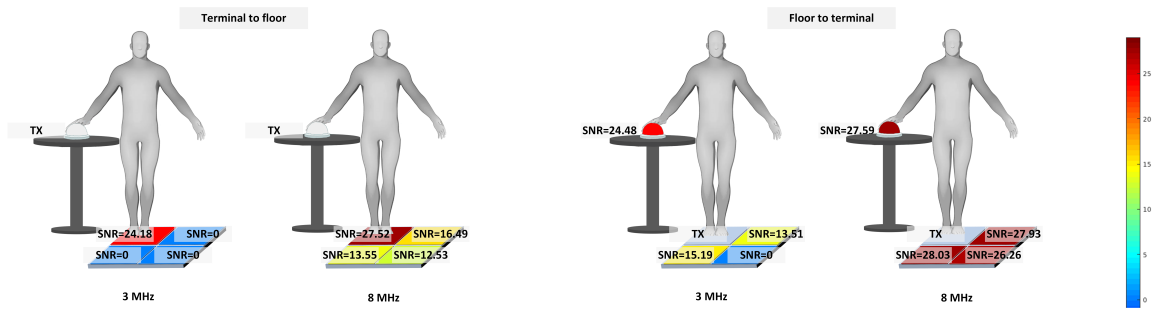


Fig. 18. Evaluation of the BCC terminal (placed on a wooden table) and BCC tile communication: both data transfer direction is evaluated on 3 MHz and on 8 MHz as well. The user is not instrumented with any wristband, but is wearing shoes.

**5.8.2 Multiple users.** As a preliminary demonstration we investigate a setup that arranges a group of non-instrumented users to form a chain that connects two BCC devices. Each participant holds his or her neighbor's hand, and the persons on the ends touch the BCC device. In this experiment, the connection is confirmed as long as the participants hold hands. User1 stands on the PSU-powered tile (A), covering all subtiles, while User2 stands on another tile (B). One subtile A is programmed to send one packet every 100 ms, and all the other subtiles are programmed to receive. The two tiles (with the two users) are placed approx. 1.6 m away from each other. The connection between User1 and User2 is established by User3, who stands in the middle and holds their hands. Figure 19 shows the measured data in two scenarios: in the first case, User2's tile is battery powered, while in the second case, this tile is connected to the same PSU as User1's tile. The data indicate that it is important for the system if the sender and receiver devices are galvanically connected or not. Either case, for this distance, communication is possible and data packets are sent successfully.

## 5.9 Discussion

The evaluation section covers several scenarios to demonstrate the capabilities and to explore the limitations of the interactive infrastructure system based on BCC. Sections 5.7.1 and 5.7.2 point out that the kind of foot wear influences the system performance. Generally, the thinner the sole is (or maybe even missing), the stronger is the signal. But communication (either transmission or receiving) is possible with all types of foot wear that we considered. These sections, together with results presented in Section 5.7.3, validate that the system is functional when used with shoes.

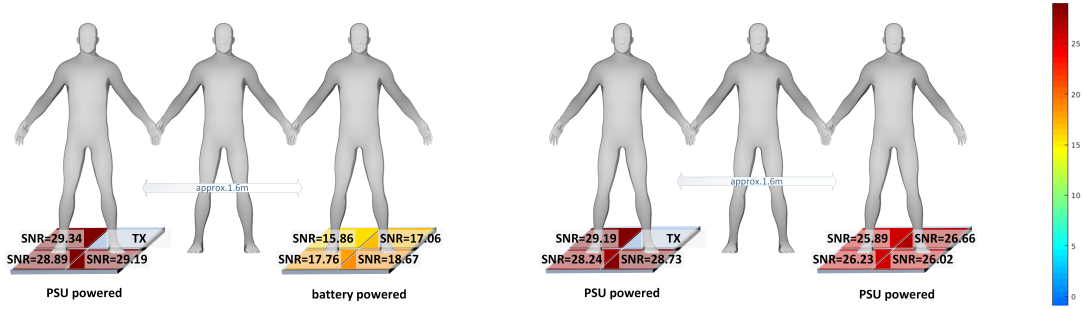


Fig. 19. SNR values while three uninstrumented user forms a chain between two tiles. One subtile is transmitting, while every other tile sensor is configured to receive.

Sections 5.7.1 and 5.7.2 show that the signal level changes with different carrier frequencies. Since the underlying BCC technology uses capacitive coupling, it is expected to see a stronger connection with higher frequencies. However, the upwards direction (sending data from the tile) generates significant over-the-air leakage if the frequency goes higher. In an application outside of a laboratory, these properties must be considered. Since Section 5.7.3 shows that 8 MHz performs well with each person (in this sample set), this frequency appears to be a practical choice. When data is sent from the tile to a wristband or to a sphere, MAC filtering can easily be added to the floor tiles' software: the software would prevent a cell from overhearing its neighbors' transmission. In the downwards direction, the electrostatic coupling is minimal, therefore the system can be used as a precise localization system even without requiring any RSSI-processing (like trilateration). So in addition to allowing communication (to send data to the wristband for storage, to change the state of the floor tiles), the system provides a path to a “room-area” localization and tracking system.

## 6 APPLICATION

We sketch now two example applications and two core services to demonstrate how the BCC infrastructure can be used for ubiquitous computing. The “ConquerIt!” application entices participants to move around in a new kind of capture game. The “MusicBand” uses the BCC sphere to invite participants for social interactions, while connecting the digital and analog world. “TrackMe” is a software module that provides a service to other applications; it records the users’ position in real time. “LightUp” is another service that sets the information stored on the wristband based on the information stored elsewhere (e.g., on the BCC-enabled sphere); when a user touches the sphere, the user’s wristband is ‘reprogrammed’ to the value stored on the sphere.

There are many scenarios that can benefit from the BCC-based technology presented here and that would use software modules like TrackMe or LightUp. Museums go through transformation while trying to engage visitors and to accommodate interactive art [17]. TouchCom can offer a new dimension for interactive museums, e.g., to explore indoors mixed-reality geocaching. Traditional geocaching is a hide-and-seek-like outdoors recreational activity. A museum may want to offer an indoor version to encourage visitors to find dedicated locations or to provide information based on the visitor’s path (cf. TrackMe) through an exhibition. As museums implement time constraints on interacting with an installation, a TouchCom-based system can record each user’s entry/exit and alert guards if a time limit is exceeded.

### 6.1 ConquerIt!

“ConquerIt!” is a lightweight proof-of-concept exertion game. We use a 4x1 setup of the BCC tiles that results in a  $160 \times 40 \text{ cm}^2$  playground. Each tile has 4 subtiles, all with several LEDs. Each user is given a wristband that

represents a specific (configurable) color. The RGB value of this color is transmitted continuously. The objective is to claim (color) tiles, either by placing a hand on a tile or by stepping on a tile. There are several possible modes to play a conquer game with this setup.

In mode #1, the subtiles randomly show up in a color, then change to another color or switch off after a few seconds. The user's goal is to touch the subtile while it still shows the user's color: the user "conquers" that field, and from then on the subtile stays with that color. This game works with any number of participants: either several users participate until all tiles have been claimed by some user, or a single-user version of the game is played against the clock (i.e., played subject to a time limit). The winner is the user with the largest number of colored tiles.

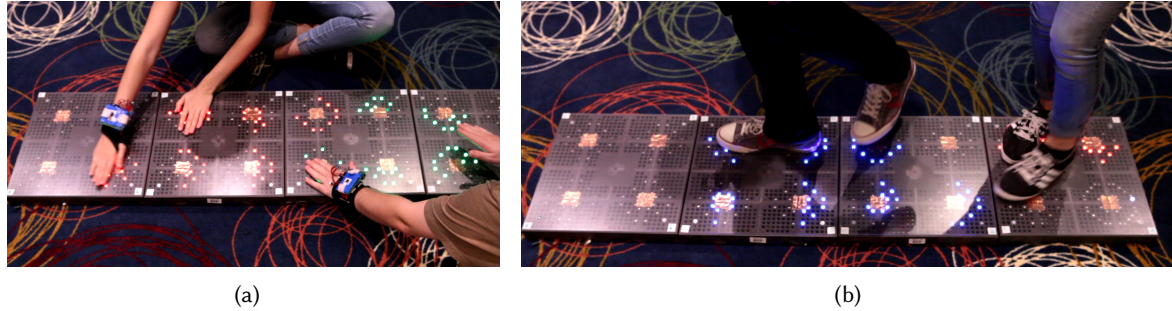


Fig. 20. ConquerIt! can be played either by touching the floor tiles by hand or by walking on them. Each subtile of the BCC floor recognizes the (instrumented) player touching it and lights up its corresponding color. The goal is to conquer as many tiles as possible.

In mode #2, the objective is to simply try to light up as many (sub)tiles simultaneously as possible. When an BCC tile sensor senses and decodes a valid packet (with a user's color), it lights up according to the given RGB value and then starts blinking for 2 sec before switching off. A user can try to keep the color on each subtile alive by continuously moving around on them. If there are several participants, then they can try to achieve the same, but now in a concurrent environment: by stepping on a blinking subtile, each user can immediately overwrite the color of that subtile. A demonstration of the ConquerIt! game can be seen in Figure 20.

## 6.2 MusicBand

The "MusicBand" application is a revised version of the "Music Arrangement" application [67]. The original game uses augmented reality to encourage music composition: the user can choose from different instruments and different music styles to create his/her own version of a given song. Each option corresponds to a physical card with an image on it, and this image serves as a visual marker. When the marker is visible for the camera of an iPad, then the corresponding virtual instrument shows up in the dedicated application and enables (plays) its music track of the song.

In the version of MusicBand presented here, instrument recognition happens through the sphere, which is connected to a tablet that shows the virtual environment. We dedicate one wristband to each instrument. Each participant is given one such wristband. When the person wearing a drum wristband touches the sphere (either with the instrumented or with the free hand), a drum shows up in the application, and the soundtrack is audible. If several persons touch the sphere at the same time, then all their instruments are present on the screen and in the song as well. The current implementation supports 3 instruments: a piano (ID 1), a drum (ID 2), and a guitar (ID 3). The size of each data field and the timing parameters for RWB are chosen as shown in Table 2.

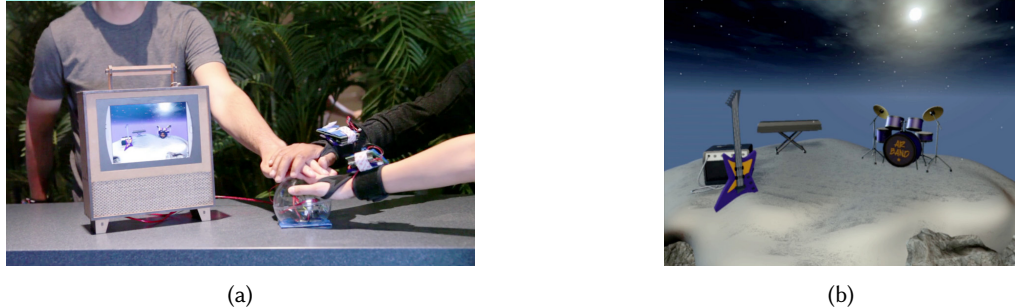


Fig. 21. MusicBand application: (a) 3 participants simultaneously touch the sphere. All transmissions are successful, consequently all corresponding instruments show up in the virtual band. (b) Snapshot of screen with the 3 instruments. See also video figure.

Figure 21a shows the MusicBand application during a demonstration. Two participants use their instrumented hand to touch the sphere, while the third participant uses his free hand. Figure 21b shows the corresponding screen recording of the tablet connected to the sphere. It can be seen that all instruments are successfully recognized. From the evaluation measurements we know that the users at this point experience connections with different quality, but the figure shows that the adaptive thresholding of the RX software successfully handles the difference in real time.

### 6.3 TrackMe

We demonstrate the “TrackMe” software module with participants that walk on a 3x3 setup of a BCC floor, which covers an area of  $120 \times 120 \text{ cm}^2$ . During the walk, each participant wears a wristband on their dominant hand. The receivers of the tiles are switched on to receive continuously; they can immediately identify the users by decoding the received packets.

Optionally, a central data collector server can be added to the system. The BCC sensors automatically connect to this server through WiFi, and each successfully received packet is timestamped and logged. Given the known position of the receiver electrodes, each packet implies that the transmitter (identified by its ID) is in close proximity (of the receiver) at the given time. Based on the information that is logged by the server, it is easy to estimate the accurate path of the user. Figure 22 shows the server’s estimations while one participant was repeating a walk 3 times.

preamble	3 byte
SFD	1 byte
PHY header	3 byte
PHY payload	1 byte
LINK protocol	RWB (no header)
LINK payload	1 byte
message length	4+4 byte
message duration	2.9257 ms
delay time	45 ms - 125 ms

Table 2. Parameters for MusicBand

preamble	3 byte
SFD	1 byte
PHY header	3 byte
PHY payload	7 byte
LINK protocol	hybrid (RWB / Aloha)
LINK payload	3 byte
message length	4+10 byte
message duration	5.1200 ms
delay time	1 s

Table 3. Parameters for LightUp

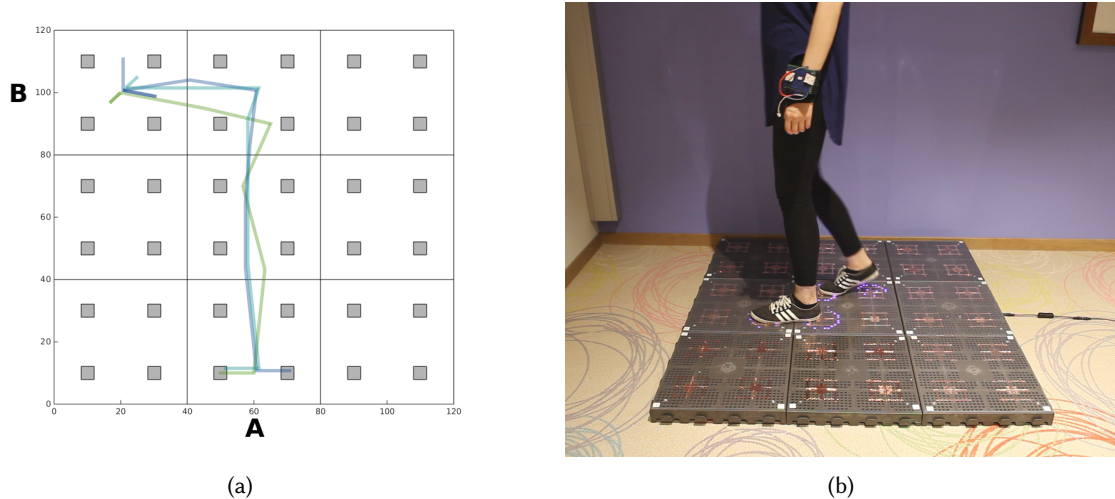


Fig. 22. TrackMe: Participant 1 walking on a path from A to B. The 3 different colors indicate the 3 different runs of the measurement campaign.

#### 6.4 LightUp

This simple service module demonstrates an application of bidirectional communication. In this setup the BCC sphere is augmented with an additional LED strip attached to it. Each LED is individually addressable and can light up in any RGB color.

In default mode, the sphere always lights up according to the message that it receives. Each wristband is programmed to broadcast its color once in each second. (Each message has a 3 byte payload that can represent an RGB value, details in Table 3). When the wristband is idle from sending, it always switches to listening mode. First, a dedicated color is used on each wristband (red, green, or blue) (Figure 23a).

For this demonstration, the sphere is connected to a phone that allows the user to switch to *recolor mode*. This mode allows a user to pick a new color for his/her wristband. When the user clicks on the 'Recolor my wristband' button, the sphere initiates a data transfer with this new RGB value to the wristband with the ID that was seen last. This wristband's ID is entered into the destination field of messages sent from the sphere. When the wristband is in listening mode and a message arrives from the sphere, the wristband overwrites the stored color value and broadcasts that color from now on (Figure 23b). In the first message with the new color it also adds an acknowledgement for the received frame. If the sphere does not see an acknowledgement for its transmitted frame in a second, it retransmits the packet, until it succeeds.

## 7 CONCLUSION

Environments with ambient intelligence must give the user a way to interact with the environment and its occupants. We have demonstrated here how body channel communication (BCC) can provide the foundation for an infrastructure that enables such environments. The core of our system is the TouchCom platform that provides a transceiver design that can be used in portable devices, mobile devices, and stationary devices as well: it is built from off-the-shelf components and pushes signal processing to the software side as far as possible.

A preliminary evaluation shows that – for a set of subjects recruited from the university community – the system works well for different persons, regardless of the characteristics of each person (including the kind of

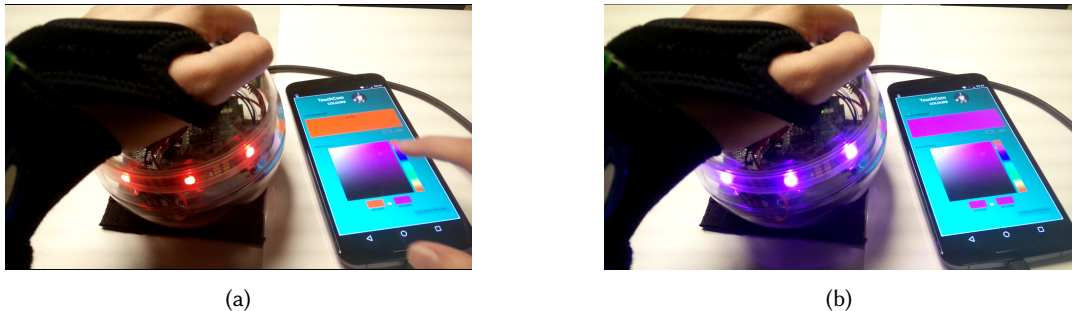


Fig. 23. LightUp: (a) The original transmitter color is red. The user selects a purple color on the smartphone connected to the sphere. (b) The sphere sent a reprogram message to the wristband, which then changes its color to purple. Each subsequent touch transmits this new color to the sphere. See also video.

foot wear chosen when using the stationary floor tile devices). Communication is possible from one device to another as well as back (at data rates that are adequate for IDs, location information, etc. but not enough to offer a substitute for video streaming).

The BCC transceivers that are placed into the floor tiles or the wristband are software-centric: like software defined radios explored in other setups, these transceivers rely on software configuration instead of employing custom hardware building blocks. The development of this interactive infrastructure was greatly facilitated by the software-centric architecture; the system can easily adapt to different environmental conditions, e.g., by setting appropriate thresholds. Flexibility is crucial for the design of future interactive infrastructures that try to integrate humans and the surrounding environment if such systems aim to support a wide range of scenarios and devices. As the cost, size, and energy consumption of digital processing elements continues to decline, a software-centric approach leverages these trends and we can look forward to systems that enable new kinds of interaction.

## REFERENCES

- [1] ICNIRP Guidelines for Limiting Exposure to Time-Varying Electric, Magnetic and Electromagnetic Fields (Up to 300 GHz). *HEALTH PHYSICS*, 74:494–522, 1998.
- [2] libopencm3 - a free/libre/open-source firmware library for various ARM Cortex-M0(+)/M3/M4 microcontrollers. Website, 11 2015. [http://libopencm3.org/wiki/Main\\_Page](http://libopencm3.org/wiki/Main_Page).
- [3] Introduction to the BodyCom Technology. Website, 09 2016. <http://ww1.microchip.com/downloads/en/AppNotes/01391A.pdf>.
- [4] Lumo Play. Website, 05 2017. <http://www.lumoplay.com/help/setup-guides>.
- [5] WizeFloor. Website, 05 2017. <https://www.wizefloor.com/index.php?Hardware/78>.
- [6] M. D. Addlesee, A. Jones, F. Livesey, and F. Samaria. The orl active floor [sensor system]. *IEEE Personal Communications*, 4(5):35–41, 1997.
- [7] M. Alwan, P. J. Rajendran, S. Kell, D. Mack, S. Dalal, M. Wolfe, and R. Felder. A smart and passive floor-vibration based fall detector for elderly. In *2006 2nd International Conference on Information Communication Technologies*, volume 1, pages 1003–1007, 2006.
- [8] J. Bae, H. Cho, K. Song, H. Lee, and H.-J. Yoo. The Signal Transmission Mechanism on the Surface of Human Body for Body Channel Communication. *Microwave Theory and Techniques, IEEE Transactions on*, 60(3):582–593, March 2012.
- [9] J. Bae, K. Song, H. Cho, H. Lee, and H.-J. Yoo. An Energy-Efficient Body Channel Communication based on Maxwell’s Equations Analysis of On-Body Transmission Mechanism. In *Medical Information and Communication Technology (ISMICT), 2012 6th International Symposium on*, pages 1–5, March 2012.
- [10] H. Baldus, S. Corroy, A. Fazzi, K. Klabunde, and T. Schenk. Human-Centric Connectivity Enabled by Body-Coupled Communications. *Communications Magazine, IEEE*, 47(6):172–178, June 2009.
- [11] A. Bränzel, C. Holz, D. Hoffmann, D. Schmidt, M. Knaust, P. Lühne, R. Meusel, S. Richter, and P. Baudisch. GravitySpace: Tracking users and their poses in a smart room using a pressure-sensing floor. In *Proceedings of the SIGCHI Conference on Human Factors in Computing Systems, CHI ’13*, pages 725–734, New York, NY, USA, 2013. ACM.
- [12] A. Braun, H. Heggen, and R. Wichert. Capfloor—a flexible capacitive indoor localization system. In *International Competition on Evaluating AAL Systems through Competitive Benchmarking*, pages 26–35. Springer, 2011.
- [13] S. Chang, S. Ham, K. Seungbum, S. Dongjun, and K. Hyunseok. Ubi-floor: Design and pilot implementation of an interactive floor system. In *2010 Second International Conference on Intelligent Human-Machine Systems and Cybernetics*, volume 2, pages 290–293, Aug 2010.
- [14] P. Dietz and D. Leigh. DiamondTouch: A multi-user touch technology. In *Proceedings of the 14th Annual ACM Symposium on User Interface Software and Technology, UIST ’01*, pages 219–226, New York, NY, USA, 2001. ACM.
- [15] A. Fazzi, S. Ouzounov, and J. van den Homberg. A 2.75mW Wideband Correlation-Based Transceiver for Body-Coupled Communication. In *IEEE International Solid-State Circuits Conference (ISSCC), 2009. Digest of Technical Papers*, pages 204–205, 2009, Feb 2009.
- [16] M. Fukumoto and M. Shinagawa. CarpetLAN: A novel indoor wireless(-like) networking and positioning system. In *UbiComp 2005: Ubiquitous Computing, 7th International Conference, UbiComp 2005, Tokyo, Japan, September 11–14, 2005, Proceedings*, pages 1–18. Springer, 2005.
- [17] S. Gilbert. Please turn on your phone in the museum. *The Atlantic*, 318(3):32–33, Oct. 2016.
- [18] N. Griffith and M. Fernström. Litefoot-a floor space for recording dance and controlling media. In *ICMC*, 1998.
- [19] K. Grønbæk, O. Iversen, K. Kortbek, K. Nielsen, and L. Aagaard. Interactive floor support for kinesthetic interaction in children learning environments. *Human-Computer Interaction—INTERACT 2007*, pages 361–375, 2007.
- [20] T. Grosse-Puppeldahl, X. Dellangnol, C. Hatzfeld, B. Fu, M. Kupnik, A. Kuijper, M. R. Hastall, J. Scott, and M. Gruteser. Platypus: Indoor localization and identification through sensing of electric potential changes in human bodies. In *Proceedings of the 14th Annual International Conference on Mobile Systems, Applications, and Services, MobiSys ’16*, pages 17–30, New York, NY, USA, 2016. ACM.
- [21] T. Grosse-Puppeldahl, S. Herber, R. Wimmer, F. Englert, S. Beck, J. von Wilmsdorff, R. Wichert, and A. Kuijper. Capacitive Near-field Communication for Ubiquitous Interaction and Perception. In *Proceedings of the 2014 ACM International Joint Conference on Pervasive and Ubiquitous Computing, UbiComp ’14*, pages 231–242, New York, NY, USA, 2014. ACM.
- [22] S. Han, H. Lim, and J. Lee. An efficient localization scheme for a differential-driving mobile robot based on rfid system. *IEEE Transactions on Industrial Electronics*, 54(6):3362–3369, Dec 2007.
- [23] P. Harikumar, M. I. Kazim, and J. J. Wikner. An analog receiver front-end for capacitive body-coupled communication. In *NORCHIP 2012*, pages 1–4, Nov 2012.
- [24] S. Helal, W. Mann, H. El-Zabadani, J. King, Y. Kaddoura, and E. Jansen. The gator tech smart house: A programmable pervasive space. *Computer*, 38(3):50–60, 2005.
- [25] M. Hessar, V. Iyer, and S. Gollakota. Enabling on-body transmissions with commodity devices. In *Proceedings of the 2016 ACM International Joint Conference on Pervasive and Ubiquitous Computing, UbiComp ’16*, pages 1100–1111, New York, NY, USA, 2016. ACM.
- [26] L. E. Hoeg and M. M. Eriksen. CapFloor: An Interactive Luminous Floor Using Capacitive Sensing. Master’s thesis, Aarhus Universitet, 2016.

- [27] C. Holz and M. Knaust. Biometric Touch Sensing: Seamlessly Augmenting Each Touch with Continuous Authentication. In *Proceedings of the 28th Annual ACM Symposium on User Interface Software & Technology*, UIST '15, pages 303–312, New York, NY, USA, 2015. ACM.
- [28] J. Hvizdos, J. Vascak, and A. Brezina. Object identification and localization by smart floors. In *2015 IEEE 19th International Conference on Intelligent Engineering Systems (INES)*, pages 113–117, Sept 2015.
- [29] O. S. Iversen, K. J. Kortbek, K. R. Nielsen, and L. Aagaard. Stepstone: An interactive floor application for hearing impaired children with a cochlear implant. In *Proceedings of the 6th International Conference on Interaction Design and Children*, IDC '07, pages 117–124, New York, NY, USA, 2007. ACM.
- [30] Y. Kado. Human-area networking technology as a universal interface. In *VLSI Circuits, 2009 Symposium on*, pages 102–105. IEEE, 2009.
- [31] P. Keyani, G. Hsieh, B. Mutlu, M. Easterday, and J. Forlizzi. Dancealong: Supporting positive social exchange and exercise for the elderly through dance. In *CHI '05 Extended Abstracts on Human Factors in Computing Systems*, CHI EA '05, pages 1541–1544, New York, NY, USA, 2005. ACM.
- [32] C. D. Kidd, R. Orr, G. D. Abowd, C. G. Atkeson, I. A. Essa, B. MacIntyre, E. Mynatt, T. E. Starner, and W. Newstetter. The aware home: A living laboratory for ubiquitous computing research. In *International Workshop on Cooperative Buildings*, pages 191–198. Springer, 1999.
- [33] L. Klack, C. Möllering, M. Ziefle, and T. Schmitz-Rode. Future care floor: a sensitive floor for movement monitoring and fall detection in home environments. In *International Conference on Wireless Mobile Communication and Healthcare*, pages 211–218. Springer, 2010.
- [34] P. Krogh, M. Ludvigsen, and A. Lykke-Olesen. "help me pull that cursor" a collaborative interactive floor enhancing community interaction. *Australasian Journal of Information Systems*, 11(2), 2004.
- [35] S. Lee, K. N. Ha, and K. C. Lee. A pyroelectric infrared sensor-based indoor location-aware system for the smart home. *IEEE Transactions on Consumer Electronics*, 52(4):1311–1317, Nov 2006.
- [36] T. Leng, Z. Nie, W. Wang, F. Guan, and L. Wang. A human body communication transceiver based on on-off keying modulation. In *International Symposium on Bioelectronics and Bioinformations 2011*, pages 61–64, Nov 2011.
- [37] Z. Lucev, I. Krois, and M. Cifrek. A Capacitive Intrabody Communication Channel from 100 kHz to 100 MHz. *Instrumentation and Measurement, IEEE Transactions on*, 61(12):3280–3289, Dec 2012.
- [38] H. H. Lund, T. Klitbo, and C. Jessen. Playware technology for physically activating play. *Artificial life and Robotics*, 9(4):165–174, 2005.
- [39] R. J. S. Matias, M. B. Cunha, A. M. Mota, and R. M. Martins. Modeling capacitive coupling systems for body coupled communications. In *Proceedings of the 7th International Conference on Body Area Networks*, BodyNets '12, pages 113–119, ICST, Brussels, Belgium, Belgium, 2012. ICST (Institute for Computer Sciences, Social-Informatics and Telecommunications Engineering).
- [40] N. Matsushita, S. Tajima, Y. Ayatsuwa, and J. Rekimoto. Wearable Key: Device for Personalizing Nearby Environment. In *Wearable Computers, The Fourth International Symposium on*, pages 119–126, Oct 2000.
- [41] L. Middleton, A. A. Buss, A. Bazin, and M. S. Nixon. A floor sensor system for gait recognition. In *Automatic Identification Advanced Technologies, 2005. Fourth IEEE Workshop on*, pages 171–176. IEEE, 2005.
- [42] J. Müller, D. Eberle, and C. Schmidt. Baselase: An interactive focus+context laser floor. In *Proceedings of the 33rd Annual ACM Conference on Human Factors in Computing Systems*, CHI '15, pages 3869–3878, New York, NY, USA, 2015. ACM.
- [43] R. J. Orr and G. D. Abowd. The smart floor: A mechanism for natural user identification and tracking. In *CHI '00 Extended Abstracts on Human Factors in Computing Systems*, CHI EA '00, pages 275–276, New York, NY, USA, 2000. ACM.
- [44] J. Paradiso, C. Abler, K.-y. Hsiao, and M. Reynolds. The magic carpet: Physical sensing for immersive environments. In *CHI '97 Extended Abstracts on Human Factors in Computing Systems*, CHI EA '97, pages 277–278, New York, NY, USA, 1997. ACM.
- [45] D. G. Park, J. K. Kim, J. B. Sung, J. H. Hwang, C. H. Hyung, and S. W. Kang. Tap: Touch-and-play. In *Proceedings of the SIGCHI Conference on Human Factors in Computing Systems*, CHI '06, pages 677–680, New York, NY, USA, 2006. ACM.
- [46] K. Partridge, B. Dahlquist, A. Veiseh, A. Cain, A. Foreman, J. Goldberg, and G. Borriello. Empirical Measurements of Intrabody Communication Performance Under Varied Physical Configurations. In *Proceedings of the 14th Annual ACM Symposium on User Interface Software and Technology*, UIST '01, pages 183–190, New York, NY, USA, 2001. ACM.
- [47] R. F. Pinkston. A touch sensitive dance floor/midi controller. *The Journal of the Acoustical Society of America*, 96(5):3302–3302, 1994.
- [48] B. Richardson, K. Leydon, M. Fernstrom, and J. A. Paradiso. Z-tiles: Building blocks for modular, pressure-sensing floorspaces. In *CHI '04 Extended Abstracts on Human Factors in Computing Systems*, CHI EA '04, pages 1529–1532, New York, NY, USA, 2004. ACM.
- [49] A.-I. Sasaki, M. Shinagawa, and K. Ochiai. Principles and Demonstration of Intrabody Communication With a Sensitive Electrooptic Sensor. *Instrumentation and Measurement, IEEE Transactions on*, 58(2):457–466, Feb 2009.
- [50] T. C. W. Schenk, N. S. Mazloum, L. Tan, and P. Rutten. Experimental Characterization of the Body-Coupled Communications Channel. In *Wireless Communication Systems (ISWCS), 2008. IEEE International Symposium on*, pages 234–239, Oct 2008.
- [51] M. Seyed, Z. Cai, and D. Lai. Characterization of Signal Propagation through Limb Joints for Intrabody Communication. *International Journal of Biomaterials Research and Engineering*, 1(2):1–12, 2011.
- [52] M. Seyed, B. Kibret, D. T. H. Lai, and M. Faulkner. A Survey on Intrabody Communications for Body Area Network Applications. *Biomedical Engineering, IEEE Transactions on*, 60(8):2067–2079, Aug 2013.
- [53] M. Shinagawa, M. Fukumoto, K. Ochiai, and H. Kyuragi. A Near-Field-Sensing Transceiver for Intrabody Communication Based on the Electrooptic Effect. *Instrumentation and Measurement, IEEE Transactions on*, 53(6):1533–1538, Dec 2004.

- [54] S.-J. Song, N. Cho, and H.-J. Yoo. A 0.2-mw 2-mb/s digital transceiver based on wideband signaling for human body communications. *IEEE Journal of Solid-State Circuits*, 42(9):2021–2033, Sept 2007.
- [55] M. Sousa, A. Techmer, A. Steinhage, C. Lauterbach, and P. Lukowicz. Human tracking and identification using a sensitive floor and wearable accelerometers. In *2013 IEEE International Conference on Pervasive Computing and Communications (PerCom)*, pages 166–171, March 2013.
- [56] P. Srinivasan, D. Birchfield, G. Qian, and A. Kidané. A pressure sensing floor for interactive media applications. In *Proceedings of the 2005 ACM SIGCHI International Conference on Advances in Computer Entertainment Technology, ACE ’05*, pages 278–281, New York, NY, USA, 2005. ACM.
- [57] M. Takahashi, C. L. Fernando, Y. Kumon, S. Takeda, H. Nii, T. Tokiwa, M. Sugimoto, and M. Inami. Earthlings attack!: A ball game using human body communication. In *Proceedings of the 2Nd Augmented Human International Conference, AH ’11*, pages 17:1–17:4, New York, NY, USA, 2011. ACM.
- [58] R. Ulyate and D. Bianciardi. The interactive dance club: Avoiding chaos in a multi-participant environment. *Computer music journal*, 26(3):40–49, 2002.
- [59] M. Valtonen, J. Maenttausta, and J. Vanhala. Tiletrack: Capacitive human tracking using floor tiles. In *2009 IEEE International Conference on Pervasive Computing and Communications*, pages 1–10, March 2009.
- [60] M. Valtonen, T. Vuorela, L. Kaila, and J. Vanhala. Capacitive indoor positioning and contact sensing for activity recognition in smart homes. *Journal of Ambient Intelligence and Smart Environments*, 4(4):305–334, 2012.
- [61] T. Vu, A. Baid, S. Gao, M. Gruteser, R. Howard, J. Lindqvist, P. Spasojevic, and J. Walling. Capacitive touch communication: A technique to input data through devices’ touch screen. *IEEE Transactions on Mobile Computing*, 13(1):4–19, 2014.
- [62] M. S. Wegmüller. *Intra-Body Communication for Biomedical Sensor Networks*. PhD thesis, ETH Zurich, 2007.
- [63] R. Xu, W. C. Ng, H. Zhu, H. Shan, and J. Yuan. Equation environment coupling and interference on the electric-field intrabody communication channel. *IEEE Transactions on biomedical engineering*, 59(7):2051–2059, 2012.
- [64] Y. Zhang, J. Zhou, G. Laput, and C. Harrison. Skintrack: Using the body as an electrical waveguide for continuous finger tracking on the skin. In *Proceedings of the 2016 CHI Conference on Human Factors in Computing Systems, CHI ’16*, pages 1491–1503, New York, NY, USA, 2016. ACM.
- [65] T. G. Zimmerman. Personal Area Networks (PAN): Near-Field Intra-Body Communication. Master’s thesis, Massachusetts Institute of Technology, 1995.
- [66] T. G. Zimmerman. Personal Area Networks: Near-field Intrabody Communication. *IBM Syst. J.*, 35(3-4):609–617, Sept. 1996.
- [67] F. Zünd, M. Ryffel, S. Magnenat, A. Marra, M. Nitti, M. Kapadia, G. Noris, K. Mitchell, M. Gross, and R. W. Sumner. Augmented creativity: Bridging the real and virtual worlds to enhance creative play. In *SIGGRAPH Asia 2015 Mobile Graphics and Interactive Applications, SA ’15*, pages 21:1–21:7, New York, NY, USA, 2015. ACM.

## APPENDIX A BODY CHANNEL COMMUNICATION

Starting with the seminal work by Zimmermann, BCC became a research topic when it was discovered that information can be propagated through the body with a modulated electric field [65, 66]. Later, Wegmüller showed that the information can be embedded either into the electric field around the human or into an electric current flowing inside the human [62]. However, one of the biggest challenges in BCC remained to provide a comprehensive model about the transmission mechanism: giving an explanation on how the electrical signals propagate inside, over, and around the human body. Various parameters should be considered including frequency, distance, transmitter/receiver couplers, or transmission power.

Since the research field of BCC is still experimental, it is consequently diverse: approaches and findings vary group by group, as Seyedi et al. concluded it in their survey [52]. Moreover, systems that use the human body as transmission channel are not only referred to as Body-Channel Communication but also as Body-Coupled Communication, Intrabody-Communication, or Human Body Communication systems. In accordance with [8], in this paper we use Body-Channel Communication (BCC) as generic term for technologies that use the human body as communication medium. In the following, we describe BCC and attempt to put all previous approaches into one taxonomy.

BCC systems can be divided into two fundamentally different approaches, depending on the prevailing electrical phenomenon of the transfer (Figure 24):

- (1) **Intrabody transmission (galvanic coupling model):** Galvanic coupling means sending an electrical signal through body tissues [62]. The model constructs an electrical circuit, considering the different body cells as different circuit elements. Intrabody transmission usually works with low frequencies (typically 10 kHz - 10 MHz) for the signal to be able to bypass the skin effect and to enter into the human body. A primary current flow appears between the two closely placed electrodes of the TX attached to the skin. This current induces a secondary current flow throughout the whole body: forming a return path - closing the circuit. Placing another pair of electrodes on the body forms an RX that is able to intercept and interpret the current change. As the electrical circuit is closed entirely inside the body, the system is not dependent on any external ground. Figure 24a depicts this model of transmission.
- (2) **Extrabody transmission (through electric fields):** Extrabody transmission means sending information through a modulated electric field on the surface and / or around the body. The transmission mechanism can be modeled with the following methods (based on the frequency used):
  - (a) **Capacitive coupling model** can be applied if the frequency is less than tens of MHz (typically 100 kHz - 40 MHz). The name emphasizes that the underlying electrical model contains several capacitive connections: between the body and the TX, between the body and the RX, between the TX and an external ground, between the RX and that same external ground, and so on [66]. This model considers the human body as one (atomic) node in the circuit. This assumption can be made because the electric field behaves as a quasi-static near-field in the considered frequency range [8]. The full circuit is always closed via the environment. Consequently, using shared grounding for the TX and the RX is vital for the system to work. Figure 24b depicts this approach.
  - (b) **Wave propagation model** can be applied if the frequency is larger than tens of MHz (typically 40 MHz - 200 MHz) [8]. In this frequency range the electrical signal propagates on the surface of the human body (far-field propagation), and the signal is attenuated with distance. This model considers the TX and the RX as special antennas, but in contrast to conventional RF approaches, the electromagnetic waves are primarily not radiating over the air, but they stay on the surface of the human body. Figure 24c shows this model.
  - (c) **Comprehensive model** can be derived from the Maxwell equations [8] and can be applied for the whole 100 kHz - 1 GHz frequency range. The model explains why different phenomena (space waves,

surface far-field propagation, reactive induction-field radiation, quasi-static near-field coupling) become dominant at different frequencies.

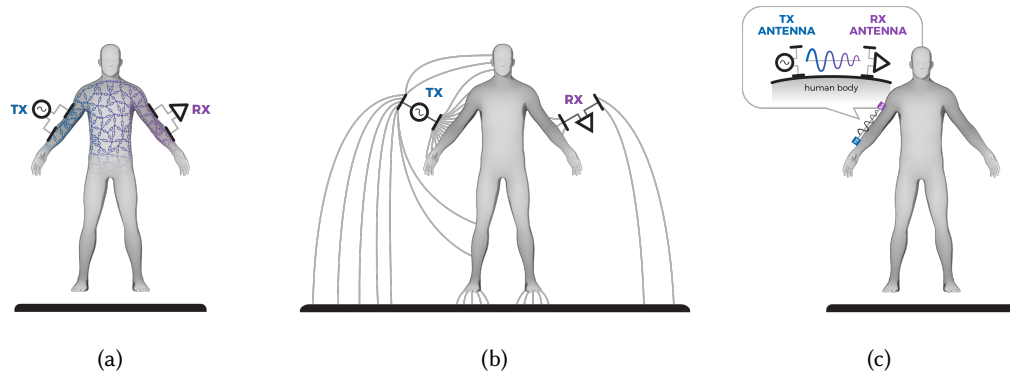


Fig. 24. 24a Intrabody transmission with galvanic coupling model; 24b EM field transmission with capacitive coupling model; 24c EM field transmission with wave propagation model.

Received May 2017; revised August 2017; accepted October 2017